ACTA OECOLOGICA 33 (2008) 324–344

available at www.sciencedirect.com

ScienceDirect

journal homepage: www.elsevier.com/locate/actoec

Original article

Competition patterns among phytoplankton functional groups: How useful are the complex mathematical models?

*Jingyang Zhao, Maryam Ramin, Vincent Cheng, George B. Arhonditsis**

Department of Physical & Environmental Sciences, University of Toronto, 1265 Military Trail, Toronto, Ontario, Canada M1C 1A4

ARTICLE INFO

Article history:
Received 10 September 2007
Accepted 11 January 2008
Published online 17 March 2008

Keywords:
Phytoplankton community
Complex mathematical models
Physiological adaptations
Resource competition
Functional grouping
Ecosystem resilience
Ecological diversity

ABSTRACT

Simple models have significant contribution to the development of ecological theory. However, these minimalistic modeling approaches usually focus on a small subset of the causes of a phenomenon and neglect important aspects of system dynamics. In this study, we use a complex aquatic biogeochemical model to examine competition patterns and structural shifts in the phytoplankton community under nutrient enrichment conditions. Our model simulates multiple elemental cycles (org. C, N, P, Si, O), multiple functional phytoplankton (diatoms, green algae and cyanobacteria) and zooplankton (copepods and cladocerans) groups. It also takes into account recent advances in stoichiometric nutrient recycling theory, and the zooplankton grazing term is reformulated to include algal food quality effects on zooplankton assimilation efficiency. The model provided a realistic platform to examine the functional properties (e.g., kinetics, growth strategies, intracellular storage capacity) and the abiotic conditions (temperature, nutrient loading) under which the different phytoplankton groups can dominate or can be competitively excluded in oligo, meso and eutrophic environments. Based on the results of our analysis, the intergroup variability in the minimum cell quota and maximum transport rate at the cell surface for phosphorus along with the group-specific metabolic losses can shape the structure of plankton communities. We also use classification tree analysis to elucidate aspects (e.g., relative differences in the functional group properties, critical values of the abiotic conditions, levels of the other plankton community residents) of the complex interplay among physical, chemical and biological factors that drive epilimnetic plankton dynamics. Finally, our study highlights the importance of improving the mathematical representation of phytoplankton adaptive strategies for resources procurement (e.g., regulation of transport kinetics, effects of transport kinetics on the kinetics of assimilation, relationship between assimilation and growth) to effectively link variability at the organismal level with ecosystem-scale patterns.

* *Corresponding author*. Tel.: +1 416 208 4858; fax: +1 416 287 7279.
E-mail address: georgea@utsc.utoronto.ca (G.B. Arhonditsis).
1146-609X/$ – see front matter © 2008 Elsevier Masson SAS. All rights reserved.
doi:10.1016/j.actao.2008.01.007

''…It is far harder, though essential, to delineate when and where the resource competition is important, and the patterns of species composition and characteristics that result…The complexity of the tasks involved ensures that delays and dead ends will be encountered, but if the route to knowledge is circuitous, that should not discourage us from setting out on the journey'' (Grover, 1997).

1. Introduction

Unravelling patterns and mechanisms that underlie phytoplankton communities is a popular area of research for experimental as well as theoretical ecologists. Although the key topics (species richness, stability and succession, trait selection, organizational resilience) pertaining to phytoplankton assemblages are no different from those impinging upon other natural communities, the operational time scales (e.g., typical generation times of algae) are significantly shorter (Scheffer et al., 2003; Reynolds, 2006). In particular, Reynolds (1993) points out that the plankton succession sequences accommodated between two winters are comparable to the number of generations that have occurred since the Weichselian glaciation period in temperate forests. Hence, the spatiotemporal phytoplankton patterns are more discernible for a human observer and can be used to derive assembly rules or – at least – to gain insights into other ecological communities (Reynolds, 2006). A characteristic example is the study of the high species richness in phytoplankton communities for eliciting conceptual paradigms that can be used for understanding the driving forces of diversity in biological systems (Lawton, 1997). Namely, one of the most puzzling questions in ecology has been the so-called ''paradox of plankton''; the violation of Hardin's (1960) principle of competitive exclusion from the phytoplankton communities in which a large number of species can be competing for essentially the same limiting resources (light, nitrogen, phosphorus, silicon, iron, inorganic carbon, and few trace metals or vitamins) in an apparently homogeneous environment.

In a seminal paper, Hutchinson (1961) offered a first explanation to the plankton paradox by pinpointing the continuous variation in environmental conditions as the most obvious factor that induces non-equilibrium phytoplankton dynamics. Since that time, there have been several attempts to circumvent the competitive exclusion principle and to explain the species diversity of planktonic communities. The various arguments invoked can be classified into three main categories: (i) food-web interactions favour species coexistence, e.g., the interacting fluctuations of algae, consumers and other higher predators contribute to the maintenance of diversity (Paine, 1966; Hastings and Powell, 1991; Heaney et al., 1988; Boersma, 1995); (ii) resource-based competition entails tradeoffs, growth strategies (e.g., gleaners, opportunists, storage specialists) and internal responses to resource availability that lead to multispecies coexistence (Tilman, 1982; Grover, 1997); and (iii) the spatiotemporal variability, e.g., the regular annual cycle driven by the gradual change of temperature and light during the year (Sommer et al., 1986) or even the small-scale, spatial heterogeneity generated by chaotic advection (Karolyi et al., 2000), promotes diversity. Moreover, the effects of this complex interplay among physical, chemical, and biological factors on the phytoplankton community composition can be further altered by climatic perturbations such as droughts, hurricanes and floods (Padisak et al., 1993). The latter mechanism commonly referred to as disturbance can induce community restructuring or can impede succession sequences from achieving equilibrium conditions and is thought to be important in keeping algal communities diverse and dynamic (Reynolds, 1993; Litchman, 1998; Floder and Sommer, 1999).

Despite the stunning complexity of phytoplankton dynamics, much of our current understanding has been based on simple models describing food-web interactions with few differential equations. These minimalistic modeling structures focus on one of the several possible causes of a phenomenon and can generate hypotheses that would not easily be achieved intuitively (e.g., Doveri et al., 1993; Huisman et al., 1999). From a mathematical standpoint, they consist of low-dimensional parameter vectors and (under some conditions) allow for analytical solutions that make it easy to explore their behaviour (Kuznetsov, 1995; Franks, 2002). On the other hand, the adequacy of these simplistic approaches for reproducing real-world dynamics has frequently been challenged (Van Nes and Scheffer, 2005; Flynn, 2005, 2006; Le Quere, 2006). For example, aside from the traditional criticism of being crude oversimplifications with arbitrarily set levels of abstraction, Flynn (2005) recently questioned the validity of some of the assumptions made from the typical nutrient–phytoplankton–zooplankton (NPZ) models. The same study also highlighted the dysfunctionality of the simpler models and attributed part of their success to the fact that ''two (or more) wrongs do sometimes make a right''. Likewise, Le Quere (2006) contended that the current models of planktonic systems are far behind our theoretical understanding. Although the line between what is unwanted detail and what is unjustified simplification is still unclear, the aquatic ecosystem modeling community seems to be reaching a consensus with regards to the need of attaining more articulated models for further advancing ecological theory (Van Nes and Scheffer, 2005). There is a pressing demand for developing models that more effectively depict the wide array of direct and synergistic effects (trophic functionality, allelopathy, omnivory, food quality effects on trophic interactions) underlying plankton dynamics (Flynn, 2006).

Sober views in the literature still raise concerns about the dire ramifications of the increasing complexity and advice to seek parsimony rather than simplicity in modeling (Simon, 2001; Anderson, 2005). To address this controversy (simple versus complex models), there are recent attempts to bring the two worlds closer and propose strategies for improving our understanding of the way complex models generate their results (see the ''scrutinize–simplify–synthesize'' framework in Van Nes and Scheffer, 2005). In this regard, we present the integration of a complex aquatic biogeochemical model with a Monte Carlo type analysis to examine competition patterns and structural shifts in the phytoplankton community under a wide range of enrichment conditions. Our model simulates multiple elemental cycles (org. C, N, P, Si, O), multiple functional phytoplankton (diatoms, green algae and cyanobacteria) and zooplankton (copepods

and cladocerans) groups. The model provides a realistic means for examining the functional properties (e.g., kinetics, growth strategies, intracellular storage capacity) and the abiotic conditions (temperature, nutrient loading) under which the different phytoplankton groups can dominate or can be competitively excluded in oligo, meso and eutrophic environments. The probabilistic treatment of the input vector (e.g., model parameters, forcing functions) of our complex model provides the means for unravelling statistically significant patterns and gaining insights into the mechanisms shaping phytoplankton communities. Finally, we critically discuss the validity of some of the typically utilized formulations of phytoplankton resource competition strategies and underscore the need for improving their mathematical representation.

2. Methods

2.1. Aquatic biogeochemical model

2.1.1. Model description

The spatial structure of the model consists of two compartments representing the epilimnion (upper layer) and hypolimnion (lower layer) of a lake. The model simulates five biogeochemical cycles, i.e., organic carbon, nitrogen, phosphorus, silica and dissolved oxygen. The particulate phase of the elements is represented from the state variables particulate organic carbon, particulate organic nitrogen, particulate organic phosphorus, and particulate silica. The dissolved phase fractions comprise the dissolved organic (carbon, nitrogen, and phosphorus) and inorganic (nitrate, ammonium, phosphate, silica, and oxygen) forms involved in the five elemental cycles. The major sources and sinks of the particulate forms include plankton basal metabolism, egestion of excess particulate matter during zooplankton feeding, settling to hypolimnion or sediment, bacterial-mediated dissolution, external loading, and loss with outflow. Similar processes govern the levels of the dissolved organic and inorganic forms along with the bacterial mineralization and the vertical diffusive transport. The model also explicitly simulates denitrification, nitrification, heterotrophic respiration, and the water column–sediment exchanges. The external forcing encompasses river inflows, precipitation, evaporation, solar radiation, water temperature, and nutrient loading. The reference conditions for our Monte Carlo analysis correspond to the average epilimnetic/hypolimnetic temperature, solar radiation, and vertical diffusive mixing in Lake Washington (Arhonditsis and Brett, 2005a,b; Brett et al., 2005). Similar strategy was also followed with regards to the reference conditions for the hydraulic and nutrient loading. Specifically, the hydraulic renewal rate in our hypothetical system was 0.384 $year^{-1}$, the fluvial and atmospheric total nitrogen inputs were 1114×10^3 kg $year^{-1}$, and nitrate and ammonium loading supplies were 561 and 34×10^3 kg $year^{-1}$, respectively. The exogenous total phosphorus loading contributed approximately 74.9×10^3 kg $year^{-1}$, while 23.9 and 17.3×10^3 kg $year^{-1}$ were entering the system as dissolved phosphorus and phosphate. In our analysis, the average input nutrient concentrations for the oligo, meso, and eutrophic environments corresponded to 50 (484 μg TN/L and 32.5 μg TP/L), 100 (967 μg TN/L and 65 μg TP/L), and 200% (1934 μg TN/L and 130 μg TP/L) of the reference conditions, respectively. Detailed model description has been provided in Arhonditsis and Brett (2005a); thus, our focus here is on the model equations pertaining to phytoplankton dynamics (Table 1).

The phytoplankton production and losses are governed by growth, basal metabolism, herbivorous zooplankton grazing, settling to sediment or hypolimnion, epilimnion/hypolimnion diffusion exchanges, and outflow losses. Nutrient, light, and temperature effects on phytoplankton growth are considered using a multiplicative model (Jorgensen and Bendoricchio, 2001). Phytoplankton growth temperature dependence ($f_{temperature}$) has an optimum level (T_{opt}) and is modelled by a function similar to a Gaussian probability curve (Cerco and Cole, 1994):

$$f_{temperature} = \exp\left(-KTgr1(T_{opt}-T)^2\right) \quad \text{when } T \le T_{opt}$$
$$= \exp\left(-KTgr2(T-T_{opt})^2\right) \quad \text{when } T > T_{opt} \tag{1}$$

We used a fairly simple mathematical model to describe the effects of nutrient limitation on phytoplankton growth ($f_{nutrient}$), which has conceptual similarities to Grover's (1991) variable-internal-stores (VIS) model. Phosphorus and nitrogen dynamics within the phytoplankton cells account for luxury uptake, and phytoplankton uptake rates depend on both intracellular and extracellular nutrient concentrations (Schladow and Hamilton, 1997; Arhonditsis et al., 2002).

$$f_{nutrient} = \min\left\{\frac{N-N_{min}}{N_{max}-N_{min}}, \frac{P-P_{min}}{P_{max}-P_{min}}\right\} \tag{2}$$

$$\frac{dN}{dt} = N_{up}N_{fb} - growth \times N \quad \frac{dP}{dt} = P_{up}P_{fb} - growth \times P \tag{3}$$

$$growth = growth_{max} f_{nutrient} f_{light} f_{temperature} \tag{4}$$

$$N_{up} = N_{upmax}\frac{DIN}{DIN+KN} \quad P_{up} = P_{upmax}\frac{PO_4}{PO_4+KP} \tag{5}$$

$$N_{fb} = \frac{N_{max}-N}{N_{max}-N_{min}} \quad P_{fb} = \frac{P_{max}-P}{P_{max}-P_{min}} \tag{6}$$

where N, P represent the intracellular nitrogen (mg N mg C^{-1}) and phosphorus (mg P mg C^{-1}) levels, DIN and PO_4 correspond to dissolved inorganic nitrogen (mg N m^{-3}) and phosphate (mg P m^{-3}) concentrations in the water column. Silica limitation on diatom growth is also accounted for by a similar submodel, while the inorganic carbon required for algal growth is assumed to be in excess and therefore is not considered by the model.

Amongst the variety of mathematical formulations relating photosynthesis and light intensities (Jassby and Platt,

Table 1 – Definitions and statistical distributions assigned to 14 model parameters pertaining to phytoplankton dynamics

Model parameter	Symbol	Unit measurement	Diatoms	Green Algae	Cyanobacteria	Sources
Maximum growth rate	$growth_{max}$	day^{-1}	N(2.2, 0.09^2)	N(1.8, 0.13^2)	N(1.2, 0.13^2)	Reynolds (2006), Jorgensen et al. (1991), Cerco and Cole (1994 and references therein), Hamilton and Schladow (1997 and references therein), Omlin et al. (2001), Chen et al. (2002 and references therein), Arhonditsis and Brett (2005a)
Basal metabolism rate	bm_{ref}	day^{-1}	N(0.10, 0.017^2)	N(0.08, 0.009^2)	N(0.08, 0.009^2)	Reynolds (2006), Jorgensen et al. (1991), Cerco and Cole (1994 and references therein), Hamilton and Schladow (1997 and references therein), Omlin et al. (2001), Arhonditsis and Brett (2005a)
Half-saturation constant for nitrogen uptake	KN	$mg\,N\,m^{-3}$	N(65, 4.3^2)	N(45, 4.3^2)	N(25, 4.3^2)	Reynolds (2006), Jorgensen et al. (1991), Cerco and Cole (1994 and references therein), Hamilton and Schladow (1997 and references therein), Arhonditsis and Brett (2005a)
Half-saturation constant for phosphorus uptake	KP	$mg\,P\,m^{-3}$	N(6, 0.9^2)	N(10, 0.9^2)	N(18, 2.1^2)	Reynolds (2006), Jorgensen et al. (1991), Cerco and Cole (1994 and references therein), Hamilton and Schladow (1997 and references therein), Omlin et al. (2001), Chen et al. (2002 and references therein), Arhonditsis and Brett (2005a)
Light attenuation coefficient for chlorophyll	$K_{EXTchla}$	$m^2\,mg\,chla^{-1}$	N(0.02, 0.004^2)	N(0.02, 0.004^2)	N(0.05, 0.009^2)	Hamilton and Schladow (1997 and references therein), Arhonditsis and Brett (2005a)
Settling velocity	$V_{settling}$	$m\,day^{-1}$	N(0.35, 0.030^2)	N(0.20, 0.052^2)	N(0.02, 0.004^2)	Reynolds (2006), Cerco and Cole (1994 and references therein), Arhonditsis and Brett (2005a), Sandgren (1991), Wetzel (2001)
Maximum nitrogen uptake rate	N_{upmax}	$mg\,N\,mg\,C^{-1}\,day^{-1}$	N(0.08, 0.009^2)	N(0.12, 0.009^2)	N(0.16, 0.009^2)	Jorgensen et al. (1991), Hamilton and Schladow (1997 and references therein), Arhonditsis and Brett (2005a)
Maximum intracellular nitrogen quota	N_{max}	$mg\,N\,mg\,C^{-1}$	N(0.20, 0.02^2)	N(0.20, 0.02^2)	N(0.20, 0.02^2)	Jorgensen et al. (1991), Hamilton and Schladow (1997 and references therein), Arhonditsis and Brett (2005a)
Minimum intracellular nitrogen quota	N_{min}	$mg\,N\,mg\,C^{-1}$	N(0.055, 0.011^2)	N(0.055, 0.011^2)	N(0.055, 0.011^2)	Jorgensen et al. (1991), Hamilton and Schladow (1997 and references therein), Arhonditsis and Brett (2005a)
Maximum phosphorus uptake rate	P_{upmax}	$mg\,P\,mg\,C^{-1}\,day^{-1}$	N(0.013, 0.001^2)	N(0.010, 0.001^2)	N(0.007, 0.001^2)	Jorgensen et al. (1991), Hamilton and Schladow (1997 and references therein), Arhonditsis and Brett (2005a)
Maximum intracellular phosphorus quota	P_{max}	$mg\,P\,mg\,C^{-1}$	N(0.029, 0.003^2)	N(0.029, 0.003^2)	N(0.029, 0.003^2)	Jorgensen et al. (1991), Hamilton and Schladow (1997 and references therein), Arhonditsis and Brett (2005a)
Minimum intracellular phosphorus quota	P_{min}	$mg\,P\,mg\,C^{-1}$	N(0.009, 0.003^2)	N(0.009, 0.003^2)	N(0.009, 0.003^2)	Jorgensen et al. (1991), Hamilton and Schladow (1997 and references therein), Arhonditsis and Brett (2005a)
Effect of temperature below optimal temperature	KTgr1	$C^{\circ -2}$	U(0.0035, 0.0045)	U(0.0045, 0.0055)	U(0.0055, 0.0065)	Reynolds (2006), Jorgensen et al. (1991), Cerco and Cole (1994 and references therein), Omlin et al. (2001), Arhonditsis and Brett (2005a)
Effect of temperature above optimal temperature	KTgr2	$C^{\circ -2}$	U(0.0035, 0.0045)	U(0.0045, 0.0055)	U(0.0055, 0.0065)	Reynolds (2006), Jorgensen et al. (1991), Cerco and Cole (1994 and references therein), Omlin et al. (2001), Arhonditsis and Brett (2005a)

1976), we used Steele's equation along with Beer's law to scale photosynthetically active radiation to depth (f_{light}):

$$f_{light} = \frac{2.718 \times FD}{K_{EXT} \times depth}(\exp(a) - \exp(b))$$

$$a = -\frac{I_{dt}}{FD \times I_{opt}} \exp(-K_{EXT} \times (ZD + depth))$$

$$b = -\frac{I_{dt}}{FD \times I_{opt}} \exp(-K_{EXT} \times ZD) \quad (7)$$

$$K_{EXT} = I_O(K_{EXTback} + K_{EXTchla}chla) \quad (8)$$

$$I_{opt} = (0.7 \times I_{dt} + 0.2 \times I_{dt-1} + 0.1 \times I_{dt-2}) \exp(-K_{EXT} \times D_{opt}) \quad (9)$$

where K_{EXT} represents the extinction coefficient (m^{-1}) determined as the sum of the background light attenuation and attenuation due to chlorophyll *a*; depth represents the epilimnion/hypolimnion depth (m); FD is the fractional day length ($0 \leq FD \leq 1$); ZD is the distance from water surface to top of the model segment (m); I_{dt} represents the daily illumination at water surface and model day *t* (Langleys day^{-1}); I_{opt} represents the optimal illumination (Langleys day^{-1}) which considers physiological adaptations by phytoplankton based on light levels during the two preceding model days I_{dt-1} and

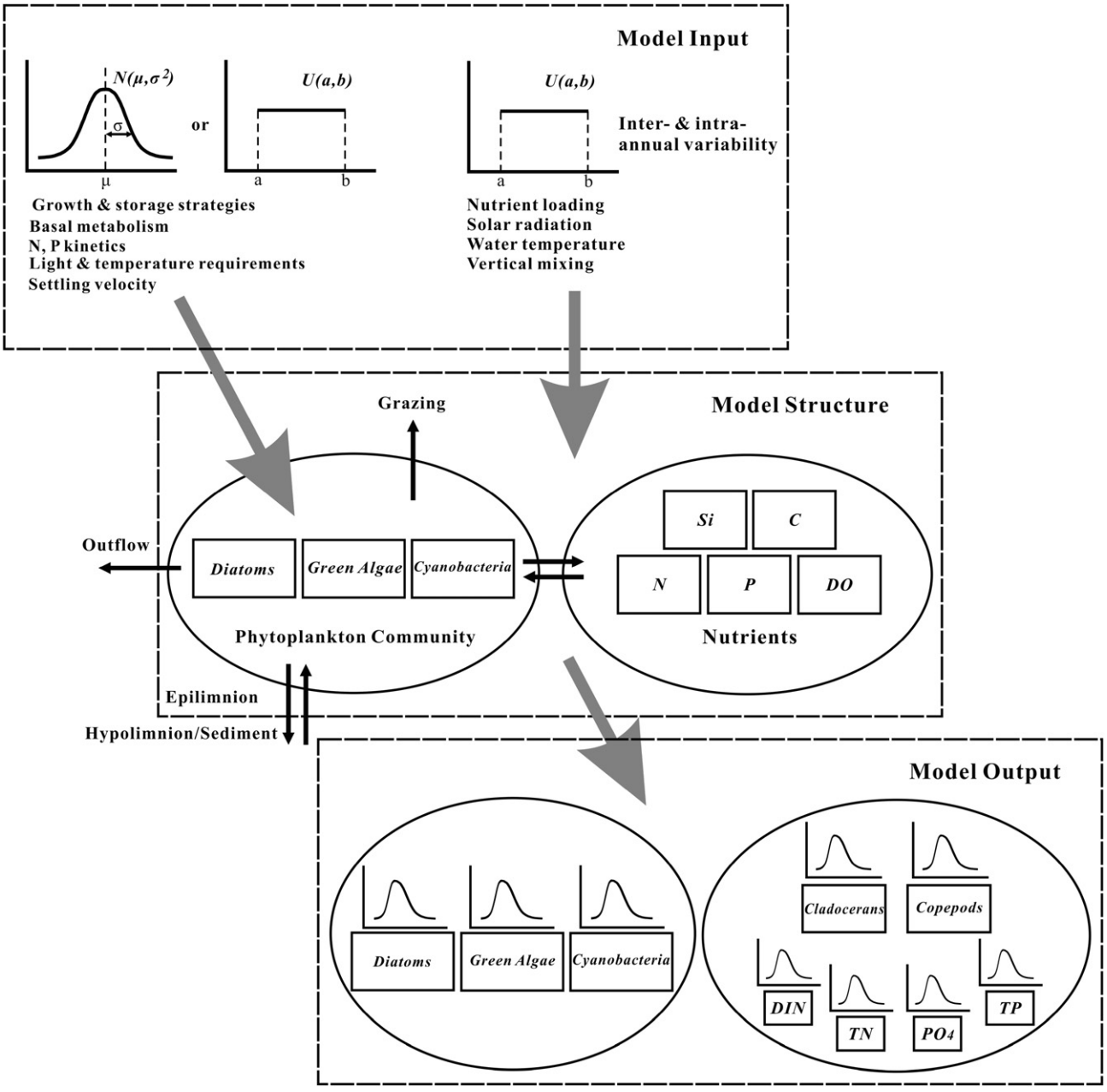

Fig. 1 – Monte Carlo analysis of the aquatic biogeochemical model. The input vector consists of forcing functions (i.e., nutrient loading, solar radiation, epilimnion temperature, hypolimnion temperature, and epilimnion/hypolimnion vertical mixing) and physiological properties (i.e., growth and storage strategies, basal metabolism, nitrogen and phosphorus kinetics, light and temperature requirements, and settling velocity) of the three phytoplankton functional groups.

I_{dt-2} (Ferris and Christian, 1991; Cerco and Cole, 1994); chl*a* is the total phytoplankton biomass expressed as chlorophyll *a* concentration ($\mu g\,L^{-1}$); D_{opt} is the depth of maximum phytoplankton production (m); and I_O represents the effects of light attenuation on the growth of the different phytoplankton groups. The latter parameter was not included in our Monte Carlo analysis, and for this presentation we used the values of the calibration vector of the model application in Lake Washington, i.e., $I_{O(diat)} = I_{O(greens)} = 1\, I_{O(cyan)} = 0.6$. Finally, phytoplankton basal metabolism is assumed to increase exponentially with temperature and corresponds to all the internal processes that decrease algal biomass (e.g., respiration and excretion) as well as natural mortality.

The three phytoplankton functional groups (diatoms, green algae, and cyanobacteria) differ with regards to their strategies for resource competition (nitrogen, phosphorus, light, temperature) and metabolic rates as well as their morphological features (settling velocity, shading effects). Diatoms are modelled as *r*-selected organisms with high maximum growth rates and higher metabolic losses, strong phosphorus and weak nitrogen competitors, lower tolerance to low light availability, low temperature optima, silica requirements, and high sinking velocities. By contrast, cyanobacteria are modelled as *K*-strategists with low maximum growth and metabolic rates, weak P and strong N competitors, higher tolerance to low light availability, low settling velocities, high temperature optima, and higher shading effects (i.e., filamentous cyanobacteria). The parameterization of the third functional group (labelled as ''Green Algae'') aimed to provide an intermediate competitor and more realistically depict the continuum between diatom- and cyanobacteria-dominated communities in our numerical experiments. In addition, the three phytoplankton groups differ with respect to the feeding preference and food quality for herbivorous zooplankton. We also note the similar distributions assigned to the nutrient quotas of the three phytoplankton groups along with the negative relationship assumed between the maximum rate of nutrient transport at the cell surface and the half-saturation constant for the same nutrient.

The herbivorous zooplankton community consists of two functional groups, i.e., cladocerans and copepods, and their biomass is controlled by growth, basal metabolism, higher predation, and outflow loss. The zooplankton grazing term explicitly considers algal food quality effects on zooplankton assimilation efficiency, and also takes into account recent advances in stoichiometric nutrient recycling theory (Arhonditsis and Brett, 2005a). The two herbivores modelled differ with regards to their grazing rates, food preferences, selectivity strategies, elemental somatic ratios, vulnerability to predators, and temperature requirements (Arhonditsis and Brett, 2005a,b). These differences drive their successional patterns along with their interactions with the phytoplankton community.

2.1.2. *Model application*

Our Monte Carlo analysis examines the functional properties (e.g., kinetics, growth strategies, and intracellular storage capacity) and the abiotic conditions (temperature, solar radiation, nutrient loading) under which the different phytoplankton groups can dominate or can be competitively excluded in oligo, meso and eutrophic environments (Fig. 1). Based on the previous characterization of the three functional groups, we assigned probability distributions that reflect our

Table 2 – Monte Carlo analysis of the model in three trophic states

	PO4 ($\mu g\,L^{-1}$)	TP ($\mu g\,L^{-1}$)	DIN ($\mu g\,L^{-1}$)	TN ($\mu g\,L^{-1}$)	TN/TP	chl*a* ($\mu g\,L^{-1}$)	DB (μg chl*a* L^{-1})	GB (μg chl*a* L^{-1})	CYB (μg chl*a* L^{-1})	CLB ($\mu g\,C\,L^{-1}$)	COB ($\mu g\,C\,L^{-1}$)
Oligotrophic											
Mean	5.2	11.2	206	304	27.4	2.1	1.4	0.6	0.1	26.1	18.7
Median	5.1	11.1	207	303	27.2	2.1	1.5	0.5	0.0	25.9	18.4
Int. range	1.4	1.8	16	16	3.8	0.4	0.4	0.5	0.1	4.8	5.7
Min	2.1	7.1	151	271	19.9	1.3	0.1	0.0	0.0	14.4	7.2
Max	10.0	16.5	244	334	40.4	3.4	2.4	2.0	2.2	46.2	39.4
Mesotrophic											
Mean	8.3	17.4	238	386	22.6	2.7	1.7	0.8	0.2	37.3	31.4
Median	7.9	17.1	237	385	22.5	2.7	1.7	0.8	0.1	37.3	31.3
Int. range	2.2	2.7	19	18	3.1	0.4	0.4	0.6	0.3	5.5	7.7
Min	3.4	10.8	180	349	10.6	0.7	0.0	0.0	0.0	9.0	3.6
Max	36.3	43.8	365	472	33.7	4.0	2.7	2.2	2.2	56.8	55.4
Eutrophic											
Mean	15.0	30.8	316	556	18.3	3.6	1.9	1.2	0.5	57.2	53.1
Median	14.8	30.6	316	556	18.2	3.6	1.9	1.2	0.5	56.9	52.5
Int. range	3.9	5.1	23	22	2.6	0.4	0.5	0.5	0.5	7.4	11.1
Min	6.1	18.2	259	506	12.7	2.6	0.4	0.0	0.0	41.7	30.3
Max	29.4	47.5	393	621	28.7	4.9	2.9	2.5	2.6	81.0	82.8

Summary statistics of the average annual values of the phosphate (PO_4), total phosphorus (TP), dissolved inorganic nitrogen (DIN), total nitrogen (TN), ratio of total nitrogen to total phosphorus (TN/TP), chlorophyll *a* (chl*a*), diatom biomass (DB), green algae biomass (GB), cyanobacteria biomass (CYB), cladoceran biomass (CLB), and copepod biomass (COB).
Mean: average value; Int. range: interquartile range (difference between the 75th and 25th percentiles); Median: median value; Max: maximum value; Min: minimum value.

knowledge (field observations, laboratory studies, literature information and expert judgment) on the relative plausibility of their growth and storage strategies, basal metabolism, nitrogen and phosphorus kinetics, light and temperature requirements, and settling velocity (Table 1). In this study, we used the following protocol to formulate the parameter distributions: (i) we identified the global (not the group-specific) minimum and maximum values for each parameter from the pertinent literature; (ii) we partitioned the original parameter space into three subregions reflecting the functional properties of the phytoplankton groups; and then (iii) we assigned normal or uniform distributions parameterized such that 95–99% of their values were lying within the identified ranges. The group-specific parameter spaces were also based on the calibration vector presented during the model application in Lake Washington (see Appendix II in Arhonditsis and Brett, 2005a). For example, the identified range for the maximum phytoplankton growth rate was 0.9–2.4 day^{-1}, while the three subspaces were 2.2 ± 0.2 day^{-1} for diatoms (calibration value $\pm$ literature range), 1.8 ± 0.3 day^{-1} for greens and 1.2 ± 0.3 day^{-1} for cyanobacteria. We then assigned normal distributions formulated such that 98% of their values were lying within the specified ranges. We also induced perturbations of the reference abiotic conditions, uniformly sampled from the range $\pm$20%, to accommodate the interannual variability pertaining to nutrient loading, solar radiation, epilimnetic/hypolimnetic temperature, and vertical diffusion. In a similar manner, we incorporated daily noise representing the intra-annual abiotic variability (Arhonditsis and Brett, 2005b). For each trophic state, we generated 7000 input vectors independently sampled from 47 (3×14 model parameters and five forcing functions) probability distributions, which then were

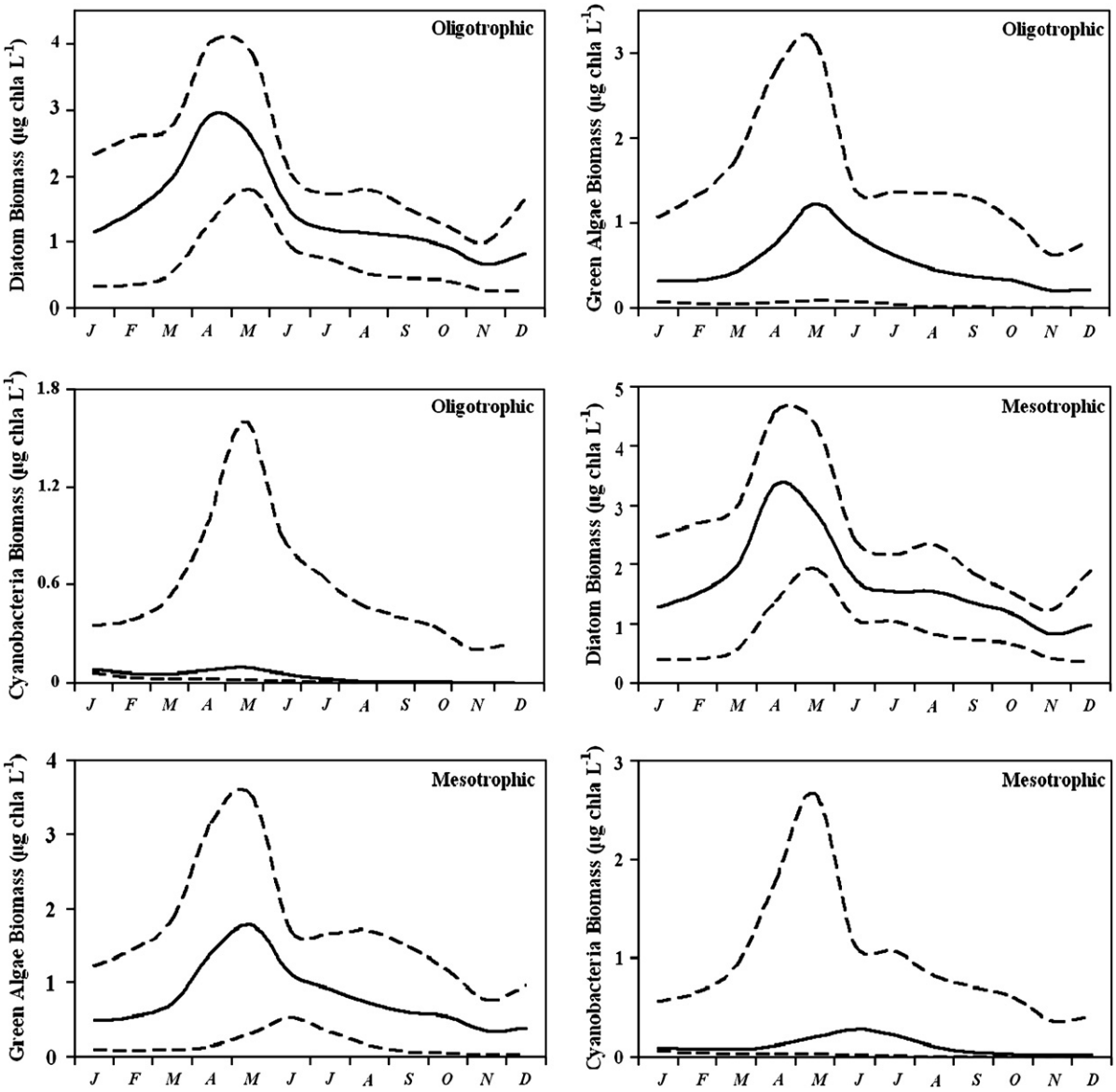

Fig. 2 – Seasonal variability of three phytoplankton functional groups (diatoms, green algae, and cyanobacteria) across a trophic gradient. Solid lines correspond to monthly median biomass values; dashed lines correspond to the 2.5th and 97.5th percentiles of the Monte Carlo runs.

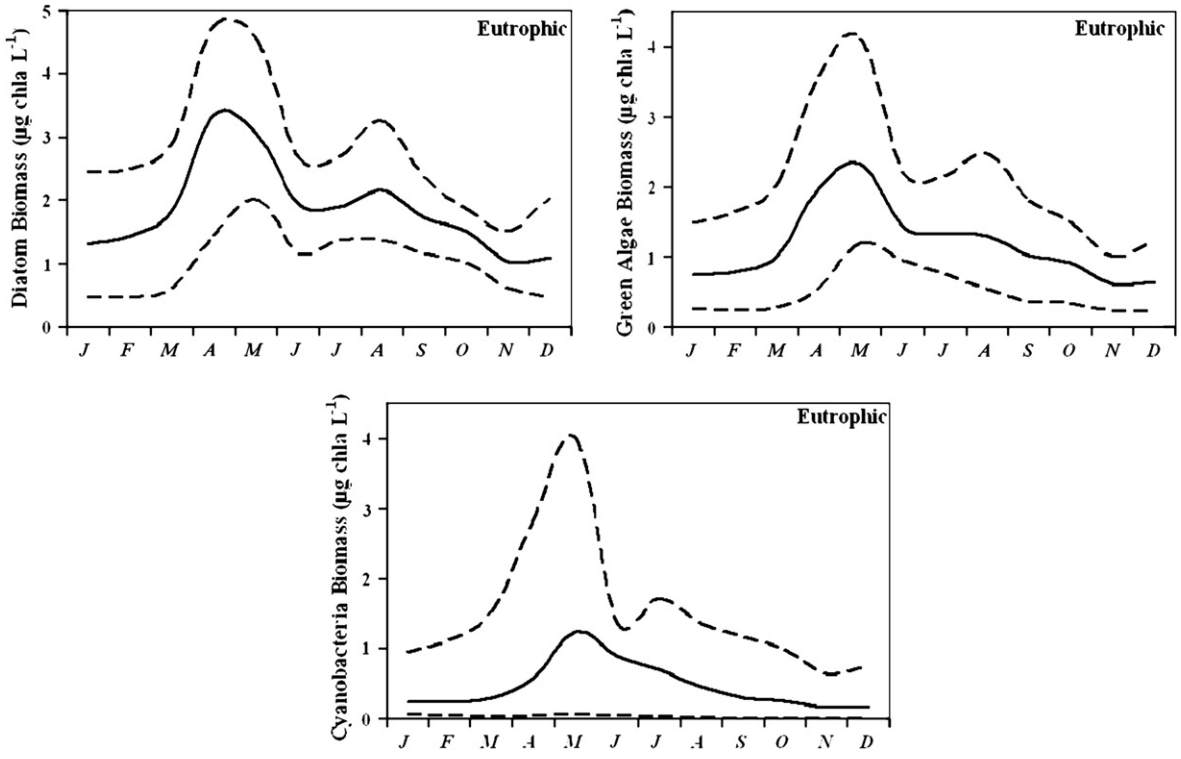

Fig. 2 – (*continued*).

used to run the model for 10 years. Finally, we generated three ($7000 \times 12 \times 9$) output matrices that comprised the average monthly epilimnetic values for the five plankton functional group biomass, dissolved inorganic nitrogen (DIN), total nitrogen (TN), phosphate (PO_4), and total phosphorus (TP) concentrations in the oligo, meso, and eutrophic environments.

2.2. *Statistical methods*

2.2.1. *Principal component analysis and multiple linear regression models*

Principal component analysis (PCA), a data reduction and structure detection technique (Legendre and Legendre, 1998), was applied for identifying different modes of intra-annual variability (Jassby, 1999; Arhonditsis et al., 2004). The basic rationale behind this application of PCA is that different phases of the intra-annual cycle may be regulated by distinct mechanisms and may therefore behave independently of each other, thereby impeding identification of clear cause–effect relationships (Jassby, 1999). For each phytoplankton functional group, the monthly biomass matrix of 12 columns (months of the year) and 7000 rows (output data sets) was formed at each trophic state; each row began with January until December. PCA was used to unravel the number of independent modes of biomass variability, and the months of year in which they were most important (component coefficients). Principal components (PCs) were estimated by singular value decomposition of the covariance matrix of the data. The selection of significant PCs was based on the Kaiser criterion, i.e., we retained only PCs with eigenvalues greater than 1. The significant modes were rotated using the normalized varimax strategy to calculate the new component coefficients (Richman, 1986). We then developed multiple linear regression models within the resultant seasonal modes of variability, whereas when a pair functional group-trophic state did not result in the extraction of significant PCs the multiple regression analysis was conducted for each month. We employed a forward-stepwise parameter selection scheme using as predictors the functional properties and abiotic conditions considered in our Monte Carlo analysis.

2.2.2. *Classification trees*

Classification trees were used to predict responses on a categorical dependent variable (i.e., phytoplankton functional groups) based on one or more independent predictor variables (i.e., model parameters, forcing functions), without specifying *a priori* the form of their interactions (Breiman et al., 1984; De'ath and Fabricius, 2000). For each functional group, we considered the July average biomass classified by lumping every 25 $\mu g\, C\, L^{-1}$ ($\approx 0.5\ \mu g\, chla\, L^{-1}$) as one class (e.g., 0–25, 25–50, and so on) to convert continuous biomass data to categorical data. The predictor variables consisted of the group-specific model parameters, the abiotic conditions, and the levels of the rest state variables in July. The outputs from the three nutrient loading scenarios were combined to obtain a matrix of 21,000 rows for the classification tree analysis. During the analysis, the algorithm began with the root (or parent) node, which corresponded to the original categorical data for each phytoplankton functional group. The data were split into increasingly homogeneous subsets with binary recursive partitioning and examination of all possible splits for each predictor variable at each node, until the Gini measure of

node impurity was below a pre-specified baseline (Breiman et al., 1984). The stopping rule for the analysis was that the terminal nodes (also known as leaves in the tree analogy) should not contain more cases than 5% of the size of each class. The final classification trees represented a hierarchical structure (shown as dendrograms) depicting the interplay among physical, chemical and biological factors that drives structural shifts in phytoplankton communities, i.e., different levels of each phytoplankton functional group (*nodes*) were associated with threshold values of its physiological features (e.g., kinetics, growth strategies, metabolic rates) along with critical levels of the abiotic conditions and the other phytoplankton competitors or zooplankton consumers (*splitting conditions*).

3. Results

3.1. Statistical results of the Monte Carlo analysis

The summary statistics of the major limnological variables in the three trophic states, as derived from averaging the model endpoints over the 10-year simulation period, are given in Table 2. The average annual phosphate (PO_4) and total phosphorus (TP) concentrations dramatically increase by nearly 180% from the oligotrophic to the eutrophic environment, whereas the corresponding dissolved inorganic nitrogen (DIN) and total nitrogen (TN) increase was relatively lower ($\leq$85%). The total nitrogen to total phosphorus ratio (TN/TP) supports stoichiometric predictions of phosphorus limitations in the three environments. However, the transition from the oligotrophic to the eutrophic state is associated with a relaxation of the phosphorus limitation as the TN/TP declines from 27.4 to 18.3; in fact, the latter environment lies close to the dichotomy boundary (Redfield ratio 16:1) between phosphorus and nitrogen limitation while several Monte Carlo simulations represented nitrogen-limiting conditions (see reported ranges in Table 1). In general, the phytoplankton biomass shows an increasing trend in response to the nutrient enrichment. Chlorophyll *a* concentrations increase from 2.1 to 2.7 and eventually to 3.6 $\mu g\,chla\,L^{-1}$. Diatoms possess superior phosphorus kinetics and therefore consistently dominate the phytoplankton community, accounting for 68, 62, and 52% of the total phytoplankton biomass at the three trophic states, respectively. Being the intermediate competitors, green algae contribute approximately 30% to the composition of phytoplankton, whereas the cyanobacteria proportion was relatively low ($\leq$15%) due to their phosphorus competitive handicap. In response to the phytoplankton biomass increase, the biomass of the two zooplankton groups progressively rises across the three trophic states, i.e., cladocerans and copepods demonstrated a twofold (from 26.1 to 57.2 $\mu g\,C\,L^{-1}$) and threefold (from 18.7 to 53.1 $\mu g\,C\,L^{-1}$) increase, respectively.

The seasonal variability of the three phytoplankton groups offers insights into the competition patterns in the three trophic environments (Fig. 2). The diatoms clearly dominate the spring bloom when their median monthly biomass varies from 2.7 to 3.3 $\mu g\,chla\,L^{-1}$. In the summer-stratified period, the diatoms also dominate the phytoplankton community, accounting for 64, 57, and 49% of the total phytoplankton biomass in the three states, respectively. Interestingly, the eutrophic environment favours the development of a secondary late summer diatom bloom ($\approx 2\ \mu g\,chla\,L^{-1}$). The seasonal patterns of the green algae are characterized by a distinct late spring–early summer increase, whereas the cyanobacteria median monthly levels remain very low ($<0.2\ \mu g\,chla\,L^{-1}$) throughout the annual cycle in the oligo and mesotrophic environments. The only exception was the eutrophic state in which the relaxation of the phosphorus limitation allows frequent exceedances of the 1.0 $\mu g\,chla\,L^{-1}$ level, and the median values remain within the 0.5–1.0 $\mu g\,chla\,L^{-1}$ range for most of the summer-stratified period. Another notable result is the ''symmetrical'' within-month variability of the diatoms and green algae (meso and eutrophic states), as indicated from the equidistant location of the monthly median relative to the 2.5th and 97.5th percentiles. In contrast, the cyanobacteria monthly variability is positively skewed, i.e., the mass of the distribution is concentrated on the abscissa and the elongated tail represents Monte Carlo simulations in which cyanobacteria gained competitive advantages and built-up their biomass.

3.2. Principal component analysis and multiple linear regression models

The PCA revealed the existence of distinct modes of variability characterizing the diatom temporal patterns (Fig. 3). In the oligotrophic environment, the first mode of variability represents the period when the lake is vertically homogeneous (January–March and November–December), and the second mode covers the period from the onset of stratification until the time when stratification begins to erode (April–October). Despite minor variations with regards to the loadings of the different months, these seasonal modes also characterize the diatom patterns in the meso and eutrophic environments. Moreover, as the external nutrient loading increases, a third significant mode is extracted, mainly associated with the diatom biomass variability in May, i.e., the period when the maximum and subsequent collapse of the spring bloom occurs, and the system enters a transient phase until the establishment of the summer stratification. Aside from the green algae in the eutrophic environment, the PCA application did not identify more than one significant PCs pertaining to the intra-annual variability of the other two functional groups.

The regression analysis intended to unveil the basic mechanisms that underlie the seasonal modes of diatom variability, using as predictor variables the phytoplankton functional properties and the abiotic conditions considered in our Monte Carlo analysis (Table 3). For each model, we present the five most significant predictors based on the absolute values of the standardized regression coefficients ($|\beta|$). The diatom basal metabolism rate (bm_{ref} (D)) is overwhelmingly the most influential parameter on the diatom variability during the cold period of the year ($|\beta| > 0.880$). The maximum diatom growth rate ($growth_{max}$ (D)) is another significant parameter positively related to the diatom biomass ($|\beta| > 0.220$). During the non-stratified period, the diatom biomass levels are also dependent on the values assigned to their maximum intracellular phosphorus quota (P_{max} (D)) and maximum phosphorus uptake rate (P_{upmax} (D)). Interestingly, being the inferior nitrogen competitors among the three phytoplankton groups, diatoms are also sensitive to the maximum nitrogen uptake rate

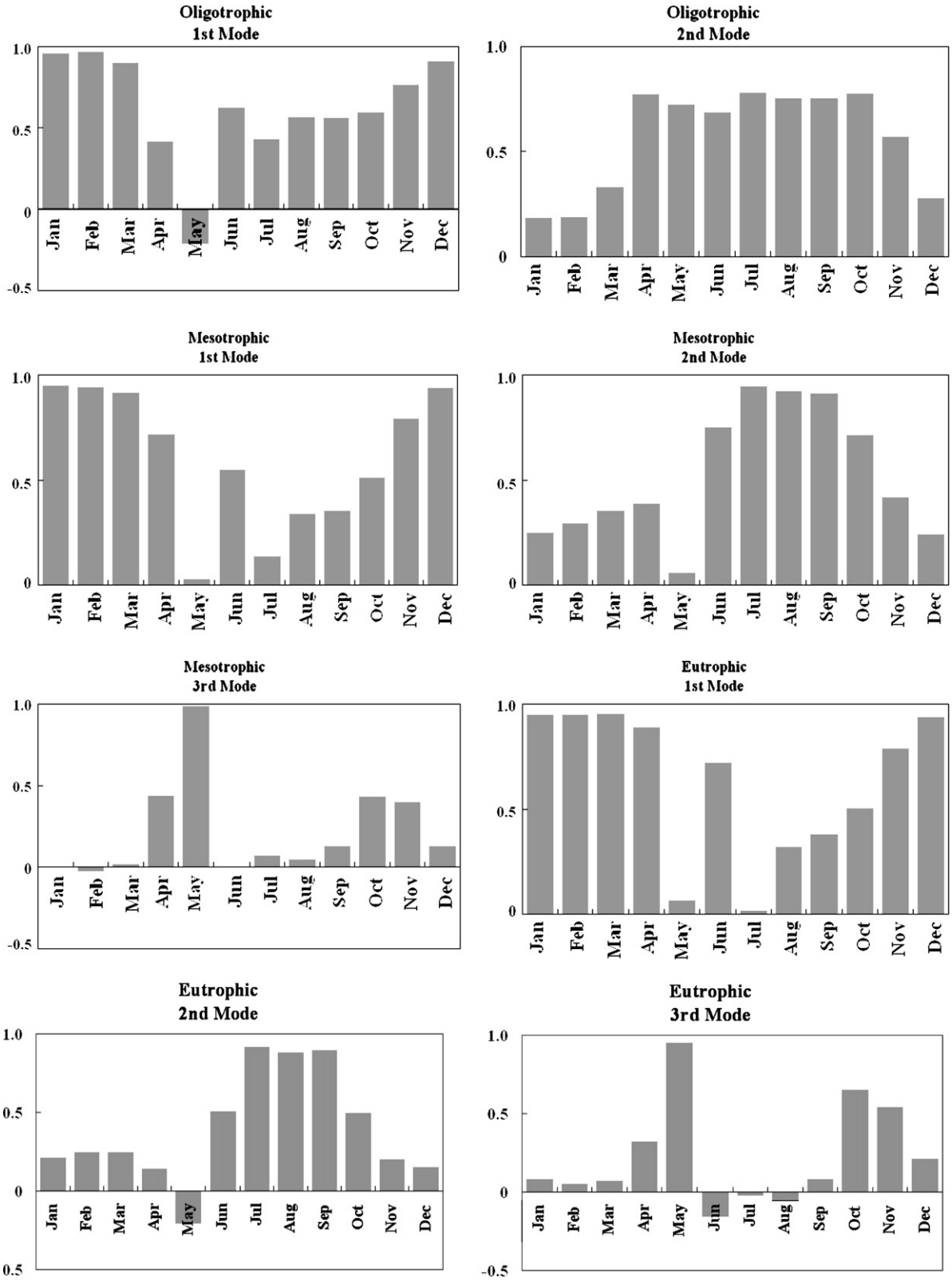

Fig. 3 – Rotated component coefficients for the principal components of diatom biomass across a trophic gradient.

(N_{upmax} (D), $|\beta| = 0.220$) and the maximum internal nitrogen (N_{max} (D), $|\beta| = 0.150$) in the eutrophic environment. The second seasonal mode (i.e., stratified period) is mainly driven by the minimum diatom phosphorus quota (P_{min} (D)), as the importance of the negative relationship between diatom biomass and P_{min} (D) was consistently highlighted at the three trophic states ($|\beta| > 0.500$). The high $|\beta|$ values of the maximum phosphorus uptake rate for the green algae (P_{upmax} (G) > 0.200)

Table 3 – Multiple regression models developed for examining the most influential factors (plankton functional properties and abiotic conditions) associated with diatom biomass in three trophic states

Oligotrophic					
First mode ($r^2 = 0.949$)	$\|\beta\|$	Second mode ($r^2 = 0.880$)	$\|\beta\|$		
bm_{ref} (D)[a]	0.820	P_{min} (D)[a]	0.738		
T_{epi}	0.231	P_{upmax} (G)[a]	0.225		
$growth_{max}$ (D)	0.225	T_{epi}[a]	0.221		
P_{max} (D)[a]	0.215	bm_{ref} (G)	0.202		
P_{upmax} (D)	0.196	Nutrient loading	0.187		
Mesotrophic					
First mode ($r^2 = 0.881$)	$\|\beta\|$	Second mode ($r^2 = 0.812$)	$\|\beta\|$	Third mode ($r^2 = 0.785$)	$\|\beta\|$
bm_{ref} (D)[a]	0.799	P_{min} (D)[a]	0.639	T_{epi}[a]	0.804
$growth_{max}$ (D)	0.258	T_{epi}	0.426	bm_{ref} (G)	0.167
KTgr1 (D)[a]	0.170	P_{upmax} (G)[a]	0.195	P_{min} (D)[a]	0.156
P_{upmax} (D)	0.169	P_{max} (D)[a]	0.186	P_{upmax} (G)[a]	0.119
P_{max} (D)[a]	0.156	bm_{ref} (G)	0.147	$growth_{max}$ (G)[a]	0.108
Eutrophic					
First mode ($r^2 = 0.922$)	$\|\beta\|$	Second mode ($r^2 = 0.866$)	$\|\beta\|$	Third mode ($r^2 = 0.891$)	$\|\beta\|$
bm_{ref} (D)[a]	0.787	T_{epi}	0.528	T_{epi}[a]	0.799
$growth_{max}$ (D)	0.268	P_{min} (D)[a]	0.501	P_{min} (D)[a]	0.212
N_{upmax} (D)	0.220	P_{max} (D)[a]	0.256	bm_{ref} (G)	0.185
KTgr1 (D)[a]	0.177	P_{upmax} (G)[a]	0.246	P_{upmax} (G)[a]	0.182
N_{max} (D)[a]	0.150	bm_{ref} (D)[a]	0.185	P_{max} (D)[a]	0.159

Symbol $|\beta|$ denotes the absolute value of the standardized coefficients.
a Negative sign of the standardized coefficients.

are indicative of the competition between the two functional groups. The epilimnetic temperature (T_{epi}) is another moderately significant predictor of the diatom variability in the three trophic environments. While the negative diatom–temperature relationship can be partly explained by the predominance of the basal metabolism losses over the net diatom growth in the oligotrophic environment during the stratified period, the switch to a positive sign when higher enrichment conditions are employed invites further investigation (see Sections 2.2.2 and 4). The third seasonal mode of variability is mainly characterized by a negative relationship with the epilimnetic temperature.

In a similar way to the diatom patterns, the two seasonal modes of green algal variability identified in the eutrophic environment represented the cold and the thermally stratified period of the system. The most significant predictors for the former period were the green algal basal metabolism (bm_{ref} (G)), maximum growth rate ($growth_{max}$ (G)), and maximum phosphorus uptake rate (P_{upmax} (G)); while the latter one was associated with the diatom basal metabolism (bm_{ref} (D)) and maximum phosphorus uptake rate (P_{upmax} (D)) along with the minimum phosphorus quota (P_{min} (G)) of the green algal cells (Table 4). Relatively similar results were also found from the monthly multiple regression models in the oligo and mesotrophic environments, i.e., the differences between the diatom and green algal growth minus metabolic loss balance control the biomass of the greens in the system. Finally, the cyanobacteria biomass variability is mainly driven from the interplay among three factors, i.e., their basal metabolic losses (bm_{ref} (CY)), the maximum rate of phosphorus transport at the cell surface (P_{upmax} (CY)), and their minimum intracellular phosphorus quota (P_{min} (CY)) (Table 5).

3.3. *Classification trees*

We developed classification trees to gain further insight into the importance of the group-specific functional properties vis-à-vis the role of lake physics, chemistry, and biology on the variability of the three phytoplankton groups during the summer-stratified period. The presented tree structures were cross-validated to avoid ‘‘overfitted’’ models, i.e., the classification tree computed from the learning sample (a randomly selected portion of the data sets) was used to predict class membership in the test sample (the remaining portion of data sets) (Breiman et al., 1984; De’ath and Fabricius, 2000). In the tree analysis of the diatom biomass, the first split into two equally sized groups is identified when the level of cladoceran biomass (CL_{Jul}) in July is 52.5 $\mu g\,C\,L^{-1}$ (Fig. 4). When $CL_{Jul} \leq 52.5\ \mu g\,C\,L^{-1}$ the diatom biomass mainly varies between 50 and 100 $\mu g\,C\,L^{-1}$ or between 1.0 and 1.5 $\mu g\,chla\,L^{-1}$ (Class 2), whereas Class 3 (1.5–2.0 $\mu g\,chla\,L^{-1}$) is dominant when $CL_{Jul} > 52.5\ \mu g\,C\,L^{-1}$. The epilimnetic temperature (T_{epi}) and zooplankton biomass are important predictors in the right branch of the tree (including 51% of original data sets). If $T_{epi} \leq 19.9\ ^{\circ}C$ most of the diatom biomass values fall in Class 3, whereas higher temperatures are associated with higher diatom biomass levels, i.e., 1.5–2.0 $\mu g\,chla\,L^{-1}$ (Class 4). Then, the diatom biomass variability was again dependent on two critical summer biomass levels of the two zooplankton groups, i.e., 71.9 $\mu g\,C\,L^{-1}$ for cladocerans and 25.4 $\mu g\,C\,L^{-1}$ for copepods (CO_{Jul}). The left portion of the tree contains 49% of the total data and the node is again separated when a cladoceran biomass threshold of 38.8 $\mu g\,C\,L^{-1}$ occurs. Although both branches are dominated by Class 2, the left node comprises lower diatom concentrations (<75 $\mu g\,C\,L^{-1}$ or 1.5 $\mu g\,chla\,L^{-1}$),

Table 4 – Multiple regression models developed for examining the most influential factors (plankton functional properties and abiotic conditions) associated with green algal biomass in three trophic states

Oligotrophic							
January ($r^2 = 0.951$)	$\|\beta\|$	April ($r^2 = 0.932$)	$\|\beta\|$	July ($r^2 = 0.796$)	$\|\beta\|$	October ($r^2 = 0.801$)	$\|\beta\|$
bm_{ref} (G)[a]	0.510	bm_{ref} (G)[a]	0.470	P_{min} (G)[a]	0.470	P_{min} (G)[a]	0.437
P_{min} (G)[a]	0.383	bm_{ref} (D)	0.422	bm_{ref} (D)	0.339	bm_{ref} (D)	0.343
bm_{ref} (D)	0.340	P_{min} (G)[a]	0.341	bm_{ref} (G)[a]	0.311	bm_{ref} (G)[a]	0.328
P_{upmax} (G)	0.311	P_{upmax} (G)	0.304	KP (D)	0.293	KP (D)	0.304
$growth_{max}$ (G)	0.246	$growth_{max}$ (G)	0.265	P_{upmax} (G)	0.262	P_{upmax} (G)	0.263
Mesotrophic							
January ($r^2 = 0.915$)	$\|\beta\|$	April ($r^2 = 0.833$)	$\|\beta\|$	July ($r^2 = 0.815$)	$\|\beta\|$	October ($r^2 = 0.777$)	$\|\beta\|$
bm_{ref} (G)[a]	0.544	bm_{ref} (G)[a]	0.467	P_{min} (G)[a]	0.460	P_{min} (G)[a]	0.413
P_{min} (G)[a]	0.326	bm_{ref} (D)	0.390	bm_{ref} (D)	0.403	bm_{ref} (D)	0.363
bm_{ref} (D)	0.325	$growth_{max}$ (G)	0.318	bm_{ref} (G)[a]	0.278	bm_{ref} (G)[a]	0.330
P_{upmax} (G)	0.318	P_{upmax} (G)	0.308	KP (D)	0.276	KP (D)	0.297
$growth_{max}$ (G)	0.312	P_{min} (G)[a]	0.286	P_{upmax} (D)[a]	0.273	P_{upmax} (G)	0.255
Eutrophic							
First mode ($r^2 = 0.926$)	$\|\beta\|$	Second mode ($r^2 = 0.894$)	$\|\beta\|$				
bm_{ref} (G)[a]	0.581	bm_{ref} (D)	0.539				
$growth_{max}$ (G)	0.477	P_{min} (G)[a]	0.435				
P_{upmax} (G)	0.314	P_{upmax} (D)[a]	0.323				
P_{max} (G)[a]	0.297	KP (D)	0.258				
KTgr1 (G)[a]	0.168	$growth_{max}$ (D)[a]	0.174				

Principal component analysis (PCA) extracted two distinct modes of variability for the eutrophic state. No distinct modes of variability were identified for the other two trophic states; therefore, the multiple regression analysis was implemented individually on each month, and herein the results of 4 months (i.e., January, April, July, and October) are presented.
Symbol $|\beta|$ denotes the absolute value of the standardized coefficients.
a Negative sign of the standardized coefficients.

Table 5 – Multiple regression models developed for examining the most influential factors (plankton functional properties and abiotic conditions) associated with cyanobacteria biomass in three trophic states

Oligotrophic							
January ($r^2 = 0.666$)	$\|\beta\|$	April ($r^2 = 0.901$)	$\|\beta\|$	July ($r^2 = 0.947$)	$\|\beta\|$	October ($r^2 = 0.969$)	$\|\beta\|$
bm_{ref} (CY)[a]	0.476	bm_{ref} (CY)[a]	0.550	P_{min} (CY)[a]	0.487	bm_{ref} (CY)[a]	0.487
P_{min} (CY)[a]	0.345	P_{upmax} (CY)	0.383	bm_{ref} (CY)[a]	0.460	P_{min} (CY)[a]	0.478
P_{upmax} (CY)	0.283	P_{min} (CY)[a]	0.343	P_{upmax} (CY)	0.393	P_{upmax} (CY)	0.371
$growth_{max}$ (CY)	0.249	$growth_{max}$ (CY)	0.341	bm_{ref} (D)	0.259	T_{epi}[a]	0.257
KP (CY)[a]	0.195	bm_{ref} (D)	0.230	KP (CY)[a]	0.254	KP (CY)[a]	0.255
Mesotrophic							
January ($r^2 = 0.820$)	$\|\beta\|$	April ($r^2 = 0.931$)	$\|\beta\|$	July ($r^2 = 0.887$)	$\|\beta\|$	October ($r^2 = 0.899$)	$\|\beta\|$
bm_{ref} (CY)[a]	0.525	bm_{ref} (CY)[a]	0.554	P_{min} (CY)[a]	0.458	P_{min} (CY)[a]	0.462
P_{min} (CY)[a]	0.376	P_{upmax} (CY)	0.401	bm_{ref} (CY)[a]	0.441	bm_{ref} (CY)[a]	0.459
P_{upmax} (CY)	0.354	P_{min} (CY)[a]	0.354	P_{upmax} (CY)	0.402	P_{upmax} (CY)	0.378
$growth_{max}$ (CY)	0.275	$growth_{max}$ (CY)	0.343	bm_{ref} (D)	0.285	bm_{ref} (D)	0.270
bm_{ref} (D)	0.240	bm_{ref} (D)	0.265	KP (CY)[a]	0.247	KP (CY)[a]	0.251
Eutrophic							
January ($r^2 = 0.953$)	$\|\beta\|$	April ($r^2 = 0.939$)	$\|\beta\|$	July ($r^2 = 0.732$)	$\|\beta\|$	October ($r^2 = 0.771$)	$\|\beta\|$
bm_{ref} (CY)[a]	0.545	bm_{ref} (CY)[a]	0.538	P_{min} (CY)[a]	0.394	P_{min} (CY)[a]	0.407
P_{upmax} (CY)	0.409	P_{upmax} (CY)	0.422	P_{upmax} (CY)	0.379	bm_{ref} (CY)[a]	0.389
P_{min} (CY)[a]	0.351	$growth_{max}$ (CY)	0.391	bm_{ref} (CY)[a]	0.357	P_{upmax} (CY)	0.359
$growth_{max}$ (CY)	0.343	P_{min} (CY)[a]	0.313	bm_{ref} (D)	0.290	bm_{ref} (D)	0.286
bm_{ref} (D)	0.274	bm_{ref} (D)	0.266	$growth_{max}$ (CY)	0.206	T_{epi}[a]	0.227

The multiple regression analysis was implemented individually on each month, and herein the results of 4 months (i.e., January, April, July, and October) are presented for comparison at each trophic state.
Symbol $|\beta|$ denotes the absolute value of the standardized coefficients.
a Negative sign of the standardized coefficients.

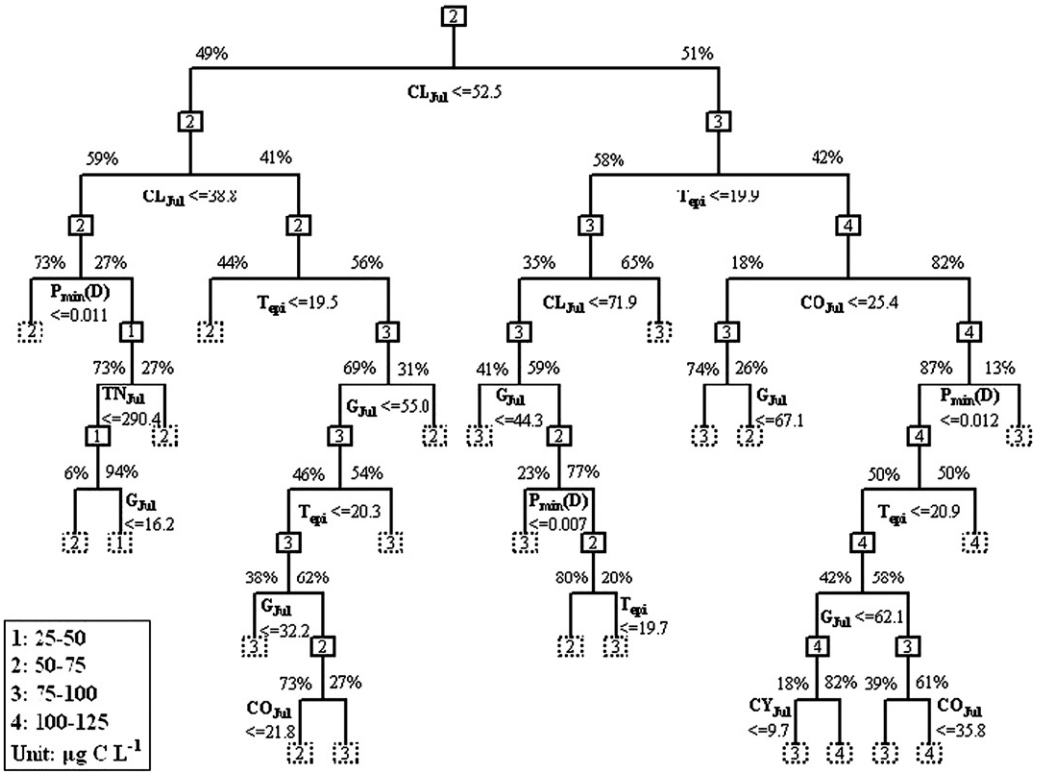

Fig. 4 – Classification tree diagram of diatom biomass under nutrient enrichment conditions. Dependent variable is the diatom biomass in July; predictors include all diatom physiological properties and the abiotic conditions along with the major limnological variables in July. Solid boxes and dashed boxes represent the split nodes and terminal nodes, respectively. The cases of the parent nodes are sent to the left child nodes if the corresponding values are no greater than the split conditions; otherwise they are sent to the right child nodes. The numbers in the boxes represent the dominant categorical dependent variable of phytoplankton-group biomass. The percentage values represent the percent of learning sample from parent nodes going to the corresponding child nodes. The cross-validation cost for this classification tree is 28.3%.

whereas the right one corresponds to higher biomass levels (>50 μg C L^{-1}). Other (relatively weak) predictors for diatoms were the minimum diatom phosphorus quota (P_{min} (D)), the total nitrogen concentrations (TN_{Jul}), and the biomass of the other two phytoplankton groups (G_{Jul} and CY_{Jul}).

The initial splitting condition for the green algae is based on the total phosphorus (TP_{Jul}) concentration, i.e., 47% of the total data set mainly dominated by Class 3 (1.0–1.5 μg chl*a* L^{-1}) concentrations is classified on the right side of the tree when $TP_{Jul} > 13.4$ μg L^{-1} (Fig. 5). This node is further subdivided when total phosphorus concentration reaches a threshold value of 25.6 μg L^{-1}. In this case, both branches are dominated by Class 3; however, if $TP_{Jul} > 25.6$ μg L^{-1} the biomass of the group labelled as ''Green Algae'' is usually higher than 75 μg C L^{-1} or 1.5 μg chl*a* L^{-1}. On the other hand, when $TP_{Jul} \leq 25.6$ μg L^{-1} the biomass of the greens varies between 0.5 and 1.5 μg chl*a* L^{-1} and a significant predictor for this subbranch of the tree is the minimum intracellular phosphorus quota (P_{min} (G) = 0.012 mg P mg C^{-1}). The left branch represents 53% of the original data sets mainly comprising biomass values within the range defined as Class 2. Subsequently, a value of P_{min} (G) > 0.010 mg P mg C^{-1} is usually associated with low green algal biomass (<1 μg chl*a* L^{-1}). When the minimum phosphorus quota is lower than this critical level, the green algae depend on the TP_{Jul} concentrations to increase their biomass (>1 μg chl*a* L^{-1}). In addition, dissolved inorganic nitrogen (DIN_{Jul}), diatom biomass (D_{Jul}), bm_{ref} (G), and P_{max} (G) act as moderately important predictors in the tree structure.

The classification tree for cyanobacteria is structurally similar to the one for green algae (Fig. 6). The first partitioning was again based on a critical total phosphorus (TP_{Jul}) concentration, the left node ($TP_{Jul} \leq 14.7$ μg L^{-1}) comprises 62% of the data set and is dominated by simulations with lower levels of cyanobacteria biomass (Class 1), while the other subset ($TP_{Jul} > 14.7$ μg L^{-1}) is mainly associated with conditions that allow cyanobacteria exceedances of the 0.5 μg chl*a* L^{-1} critical level. Based on a second critical total phosphorus concentration ($TP_{Jul} = 24.6$ μg L^{-1}), the right part of the tree is further split into two almost equal data sets. If $TP_{Jul} > 24.6$ μg L^{-1}, a maximum phosphorus transfer rate (P_{upmax} (CY)) higher than 0.0072 mg P mg C^{-1} day^{-1} usually results in cyanobacteria biomass within the Class 3 range. When $TP_{Jul} \leq 24.6$ μg L^{-1} the cyanobacteria variability is mainly driven by their metabolic loss strategies (bm_{ref} (CY)). On the left side of the tree diagram, P_{min} (CY) is a significant predictor, and a critical value of 0.007 mg P mg C^{-1} further subdivides the data set. Other influential factors of the cyanobacteria variability were the dissolved inorganic nitrogen (DIN_{Jul}) and copepod biomass (CO_{Jul}). Finally, it should be noted that the cross-validation

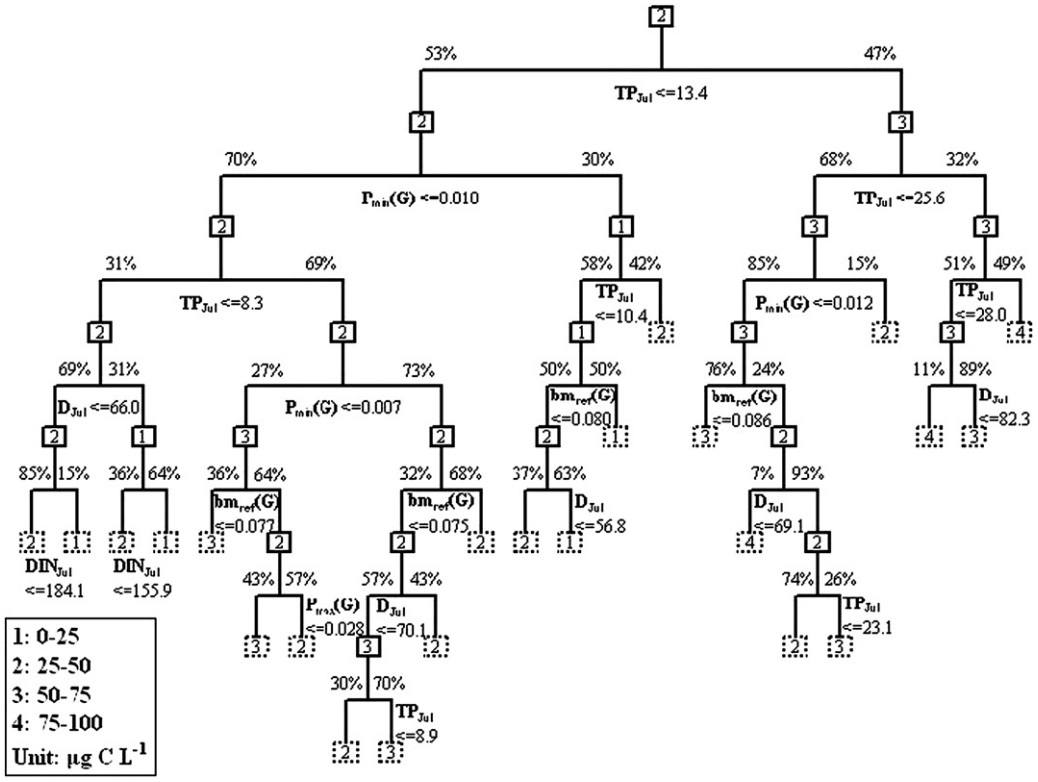

Fig. 5 – Classification tree diagram of green algal biomass under nutrient enrichment conditions. Dependent variable is the green algal biomass in July; predictors include all green algal physiological properties and the abiotic conditions along with the major limnological variables in July. The cross-validation cost for this classification tree is 38.4%.

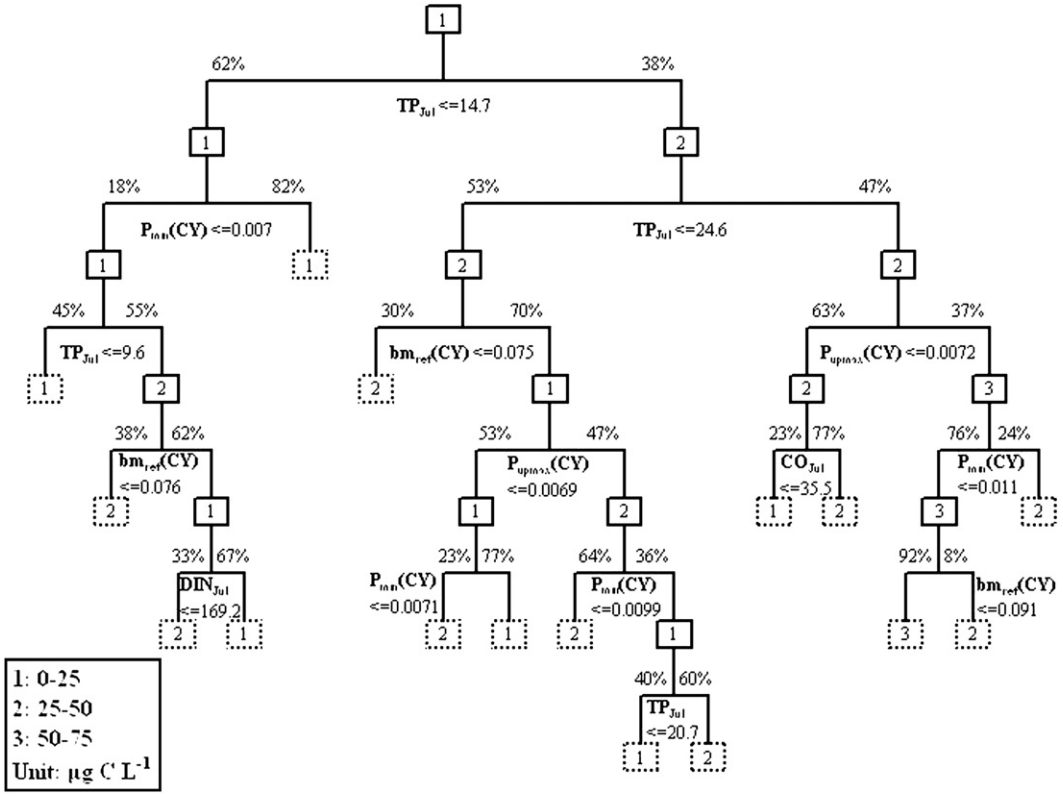

Fig. 6 – Classification tree diagram of cyanobacteria biomass under nutrient enrichment conditions. Dependent variable is the cyanobacteria biomass in July; predictors include all cyanobacteria physiological properties and the abiotic conditions along with the major limnological variables in July. The cross-validation cost for this classification tree is 22.4%.

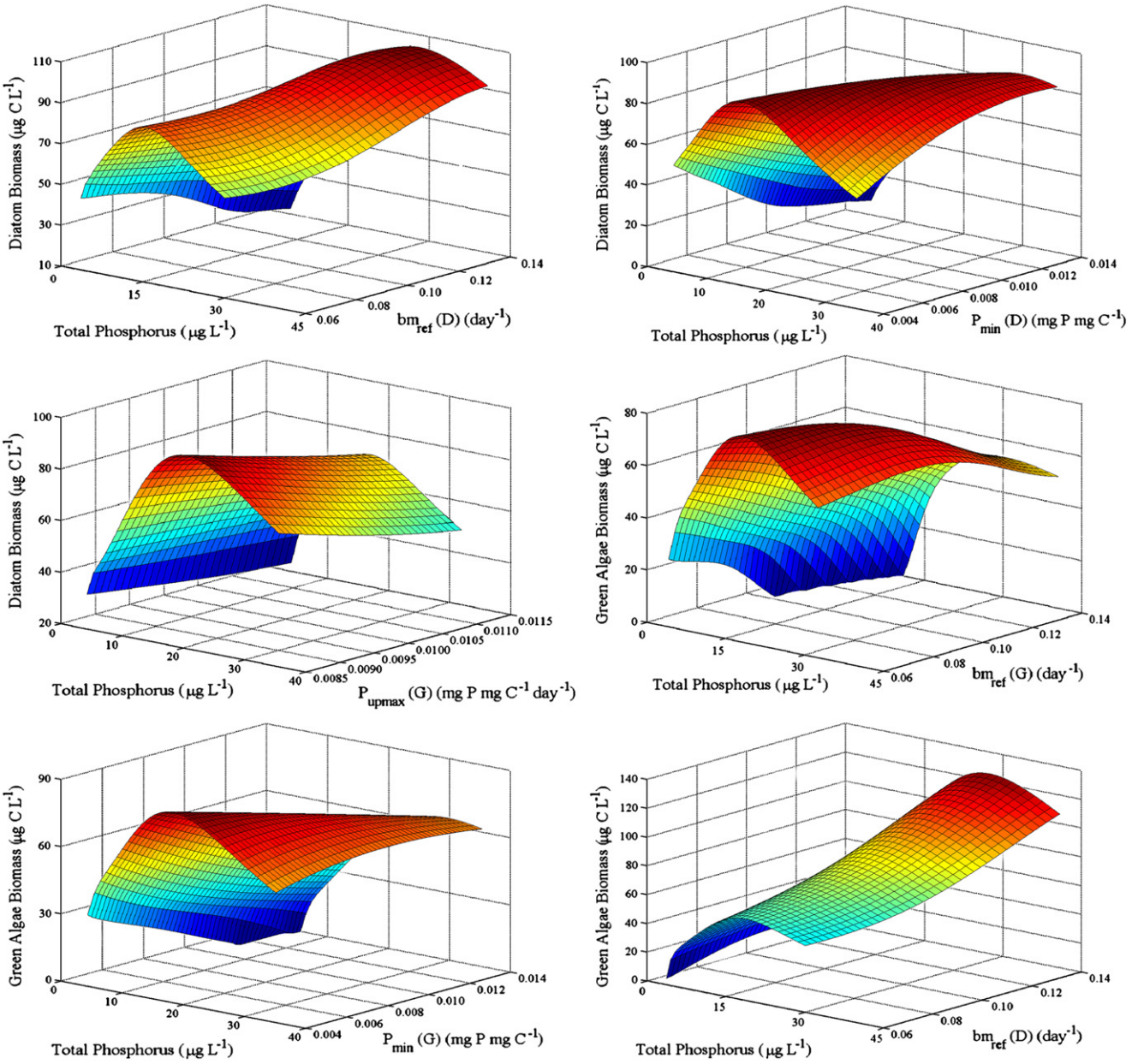

Fig. 7 – Plots of phytoplankton functional group biomass against selected physiological properties (basal metabolism, minimum phosphorus cell quota, maximum phosphorus uptake rate) and a wide range of nutrient loading that corresponds to the 1–300% of the current total organic carbon, total nitrogen and total phosphorus input concentrations in Lake Washington.

cost (i.e., an estimate of the misclassification error) for the three classification trees was 28.3, 38.4, and 22.4%, respectively.

3.4. *Examination of the role of the most influential parameters under nutrient enrichment conditions*

To analyze the impact of significant model parameters on different phytoplankton groups as identified from the multiple regression models and classification trees, we developed a special simulation procedure. Maintaining all the rest forcing functions at reference values (Arhonditsis and Brett, 2005b), a series of nutrient loadings was created spanning the 1–300% range of the reference exogenous nutrient input (or 9.7–2901 μg TN/L and 0.65–195 μg TP/L) with an increment of 1%. These enrichment conditions were used to reproduce a broad range of trophic states (i.e., from ultra-oligotrophic to hyper-eutrophic). For each nutrient loading the model was run for a 10-year period, which was sufficient a simulation period to reach ''equilibrium'' phase; i.e., the same pattern was repeated each year. The phytoplankton biomass was recorded subsequently at an arbitrarily chosen day in summer (15th, July) of the 10th year. Thereafter, we started a simulation in which one model parameter of interest (e.g., bm_{ref} (D)) was changed, and all the other parameters were kept as in the calibration vector reported in the Lake Washington presentation

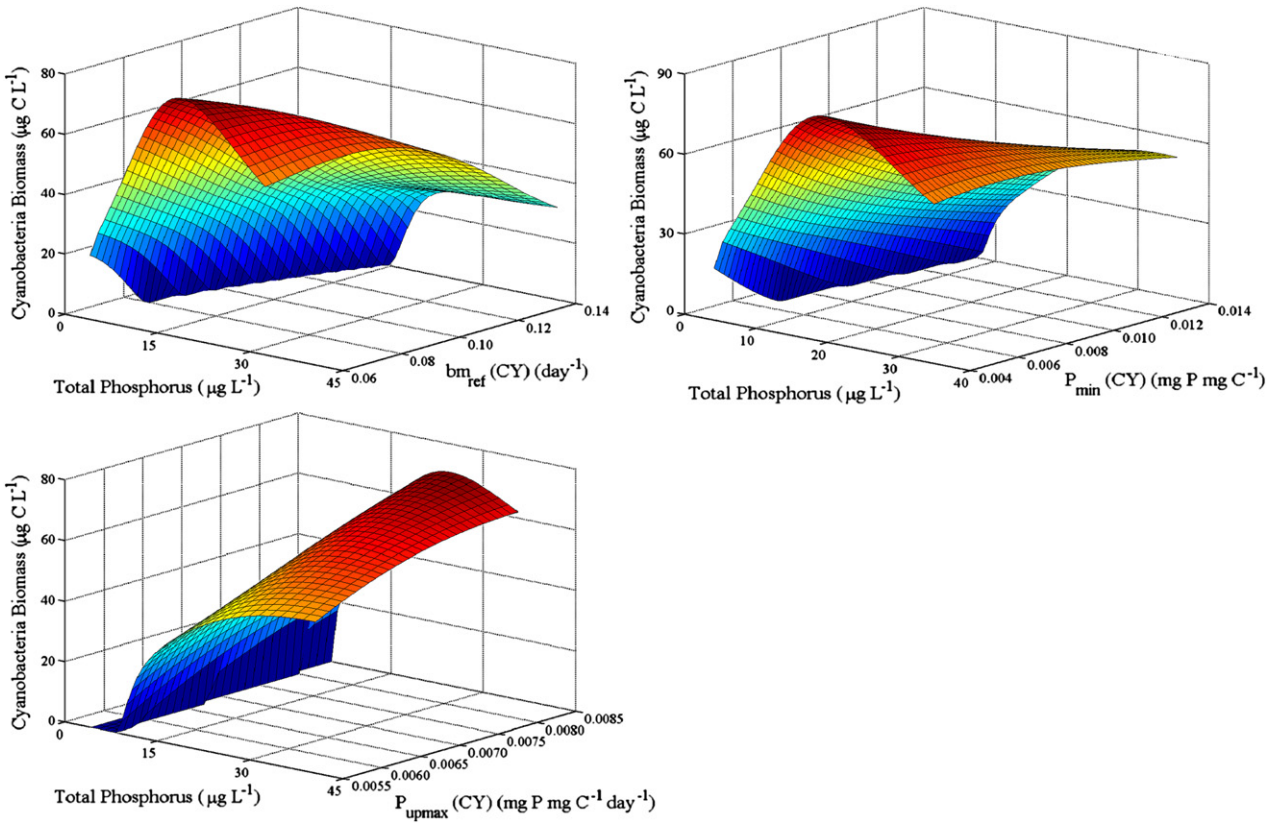

Fig. 7 – (*continued*).

(Arhonditsis and Brett, 2005a). The final state of the modelled plankton dynamics after each step was used as a new starting point for the simulation of the next step.

We selected various physiological properties (basal metabolism losses, phosphorus kinetics) of the different phytoplankton groups (i.e., bm_{ref} (D), P_{min} (D) and P_{upmax} (G) on diatoms; bm_{ref} (G), P_{min} (G) and bm_{ref} (D) on green algae; bm_{ref} (CY), P_{min} (CY) and P_{upmax} (CY) on cyanobacteria), and the resulting biomass was plotted against the corresponding parameter and nutrient loading values (Fig. 7). All nine plots almost consistently show that the phytoplankton biomass–nutrient loading relationship is characterized by a concave (concave downward) shape where the apex (maximal extremum) is usually located within the 120–180% range of the reference nutrient input. The subregion where phytoplankton biomass decreases with increasing nutrient loading probably reflects the control of herbivorous grazing on phytoplankton along with the prevalence of nitrogen-limiting conditions. The diatom biomass has a decreasing trend with respect to bm_{ref} (D) and P_{min} (G) when nutrient loading is low, but an increasing trend when loading is high. In contrast, the diatom–P_{upmax} (G) relationship is monotonically decreasing throughout the nutrient loading range. The green algal biomass monotonically decreases with increasing bm_{ref} (G) and P_{min} (D) values (especially at <200% loading levels), while the relationship with the bm_{ref} (D) is monotonically increasing and the global maxima are usually observed at the higher end of the diatom metabolic loss rates under high enrichment conditions. The cyanobacteria biomass has a negative relationship with the bm_{ref} (CY) and P_{min} (CY) and a positive one with the P_{upmax} (CY), but these patterns are weakening as the nutrient loading increases. Finally, the cyanobacteria biomass showed a discontinuous pattern with a sudden jump around the 30% level of the reference loading conditions, which corresponds to average input concentrations of 290 μg TN/L and 19.5 μg TP/L. In the context of the present model specification (e.g., parameter values, external forcing, features of the hypothetical system), this TP loading value is the critical threshold for the competitive exclusion of cyanobacteria from the system.

4. Discussion

The development of laws of simplification and aggregation is a central problem in ecology and evolutionary biology (Levin, 1992). Mathematical modeling as a tool for elucidating ecological patterns is subject to the complexity issue, and attempts to abstract the essential ecosystem features for achieving the optimal model dimension are ubiquitous in modeling practice (Levins, 1966; Costanza and Sklar, 1985; Jorgensen, 1999; Arhonditsis and Brett, 2004). Hence, it is not surprising that one of the "hottest" debates in the ecological modeling literature is the selection of the optimal aggregation level of the biotic communities; aquatic biogeochemical modeling being no exception (Anderson, 2005; Flynn, 2005; Arhonditsis et al., 2006). Despite the satisfactory predictability attained at higher aggregation levels (Scheffer et al., 2003), several

aquatic ecosystem modellers argue that there are good reasons to opt for a finer representation of the plankton communities, e.g., species populations are more sensitive to external perturbations (nutrient enrichment, episodic meteorological events), and important ecosystem functions are ultimately linked to particular plankton functional groups (Cottingham and Carpenter, 1998; Flynn, 2005; Arhonditsis et al., 2007). Others claim that the derivation of distinct functional groups from fairly heterogeneous planktonic assemblages poses challenging problems with respect to the development of robust parameterizations that can support predictions in a wide array of spatiotemporal domains (Anderson, 2005). In this study, we analyzed a complex aquatic biogeochemical model that has successfully reproduced seasonal succession plankton patterns (Arhonditsis and Brett, 2005b), and the probabilistic treatment of its input vector (e.g., model parameters, forcing functions) offered insights into the mechanisms shaping competition patterns and structural shifts in phytoplankton communities.

4.1. *Competition patterns among phytoplankton functional groups*

The crux of the functional grouping problem was articulated by Anderson (2005), who used as an example the typical representation of the wide variety of plankton groups involved in the ocean calcification by the single coccolithophore species *Emiliania huxleyi*. While a great deal of effort has been devoted to understand the conditions underlying this species dynamics (Tyrrell and Merico, 2004; Lessard et al., 2005), the anticipated improvement of its parameterization does not address the enormous variability characterizing other calcifying algal species, such as *Florisphaera profunda* and *Umbellosphaera irregularis*. Given that similar concerns can be raised for other plankton classification schemes typically used in aquatic biogeochemical modeling (e.g., picophytoplankton, nitrogen fixers, chlorophytes, dimethyl sulfide producers), is it reasonable to expect single-valued data set-specific parameter estimates of artificially defined biotic entities to be extrapolated over wider geographical regions?

In this modeling study, the within-group variability was depicted by probability distributions assigned to the three functional groups to examine the simulation robustness of seasonal succession plankton patterns in epilimnetic environments. Our analysis suggests that the reproduction of the ordered succession of seasonal events in temperate thermally stratified lakes is quite robust and can be manifested under a wide range of group-specific functional properties and abiotic conditions. However, the straightforward delineation of the modelled functional groups (diatoms, cyanobacteria, and an intermediate competitor labelled as ''Green Algae'') along with the distinct niche partitioning assumed probably made the reproduction of these patterns easier (Scheffer and Van Nes, 2006). Our numerical experiments are based on a phytoplankton community that consists of three species with very discrete positions in the multidimensional habitat simulated. Put simply, if the density of a cloud depicts niche utilization in a three dimensional space, then the centers of mass and the volumes occupied from the three clouds are distant and have minimum overlap, respectively. Being sufficiently different, the three species are able to coexist and, most importantly, exhibit the range of responses typically reported in the limnological literature (Sommer et al., 1986; Marshal and Peters, 1989; Vanni and Temte, 1990; Hansson et al., 1998; Rothhaupt, 2000). Viewed from an environmental management perspective, this admittedly simplified representation of the phytoplankton community can support predictions in the extrapolation domain without the need to invoke extra complexity.

Our analysis spanned a gradient of phosphorus-limiting conditions and therefore the competition patterns arisen can be partly explained with concepts from the algal nutritional physiology. Having the features of a velocity and phosphorus affinity specialist, diatoms are the dominant competitors and consistently account for a large portion (>50%) of the total phytoplankton biomass. Because of its high maximum growth (cell division) rate combined with high maximum phosphorus transport rate at the cell surface and low half-saturation constant, the diatom-like species was able to overcome the higher sinking loss and basal metabolism rates assigned along with the higher grazing pressure exerted from the zooplankton community (see following discussion). The diatom run-to-run variability during the summer-stratified period (second seasonal mode) was associated with the minimum intracellular phosphorus quotas, i.e., the minimum phosphorus requirement to produce another cell. This result is not surprising, as earlier work from Grover (1991) similarly showed that a decrease in the minimum nutrient quota provides competitive advantage in both equilibrium and non-equilibrium habitats. The interesting finding here is that the predominant role of this parameter on the interspecific competition is also manifested with complex models where several – often contrasting – forces (e.g., vertical mixing, herbivory, seasonal forcing) are explicitly modelled. In contrast with the minimum phosphorus quota, an increasing maximum bound on the intracellular phosphorus decreases the competitive ability in nutrient-rich habitats, such as the summer epilimnion of the eutrophic state or the period when the system is well-mixed, i.e., the first seasonal mode of variability (Table 3). In essence, the negative relationship between this parameter and the diatom biomass implies that a higher maximum rate of conversion of the intracellular nutrients into storage products/macromolecules (i.e., the fabric of organelles and other complex cellular components) results in reduced growth even when the ambient levels are relatively high. Moreover, Turpin (1988) suggested a tradeoff between the kinetics of transport and the assimilation rates arising from the limited amount of protein per cell that can be allocated between the two processes. This hypothesis has not been considered in this study, as similar distributions were assigned to the maximum nutrient quotas ($N_{max(i)}$, $P_{max(i)}$) of the three phytoplankton groups and were sampled independently from the corresponding maximum transport rates ($N_{upmax(i)}$, $P_{upmax(i)}$). While Grover's (1991) study showed that the negative relationship between the upper bound of maximum nutrient transport rate and the maximum nutrient quota can be a critical factor in non-equilibrium habitats, it is unlikely that the competition patterns reported here would have changed if we had considered this assumption.

Being assigned to neighbouring locations along the niche axis that represents the species phosphorus competitive

ability, the diatoms and the green algae directly compete against each other, as the one group's functional properties (growth rates, storage capacity, metabolic rates) and biomass levels can be significant predictors for the other one's dynamics (Tables 3 and 4; Figs. 4 and 5). On the other hand, cyanobacteria are somewhat more remotely located along the same axis, and therefore their variability remains unaffected from the other two groups' functional properties or biomass levels (Table 5; Fig. 6). The metabolism rate is another important determinant of the competitive ability of the three residents of the phytoplankton community. In this model, the phytoplankton basal metabolism rate encompasses natural mortality, respiration (i.e., oxidation of the stored organic matter to produce energy) as well as excretion (Arhonditsis and Brett, 2005a). Regarding the latter process, Baines and Pace (1991) showed that the phytoplankton exudation of organic matter can be as high as 13% of the total fixation during photosynthesis and increases nonlinearly with primary productivity with very low percentage extracellular organic matter release in eutrophic lacustrine ecosystems. The differences in the group-specific metabolic rates can overturn species competitive dominance based on the differences in physiological characteristics. In particular, the role of the metabolic losses can be particularly influential in non-steady environments where the competitive dynamics can be very slow, and thus small intergroup differences in the metabolic loss rates can easily negate competitive (dis)advantages causing structural shifts in phytoplankton communities (Grover, 1991).

4.2. *Direct and indirect relationships in the phytoplankton–zooplankton interface*

Our numerical experiments also underscore the manifold effects of the herbivores on the structure of the phytoplankton community. In particular, the third seasonal mode representing the mid-late spring diatom biomass variability in meso and eutrophic environments was mainly associated with the epilimnetic temperature (Table 3), i.e., a significant regulatory factor of the cladocerans growth in the spring (Arhonditsis et al., 2004). The latter zooplankton group is a dominant grazer that can strongly control the standing crop of the diatom-dominated spring blooms; the so-called clear water phase (Lampert and Sommer, 1997).

More intriguing was the nature of the prey–predator interactions during the summer-stratified period, and their interpretation requires invoking the role of herbivorous grazing in concert with the recycling processes. Namely, our model considers nutrient release from zooplankton excretion and during the feeding process when zooplankton homeostasis is maintained by removing elements in closer proportion to zooplankton body ratios than to the elemental ratio of the food (Elser and Foster, 1998; Arhonditsis and Brett, 2005b). The quantitative significance of these nutrient sources to phytoplankton productivity is unclear, although there is evidence that the excreted or egested nutrients from zooplankton can play an important role in the summer epilimnion (Wetzel, 2001). In our analysis, the exceedance of several critical threshold values of the summer cladoceran biomass was associated with higher diatom levels (Fig. 4), while the positive temperature $|\beta|$ values in the meso and eutrophic states probably reflect the predominant role of the temperature-dependent mineralization as a phosphate source in the epilimnetic environment (Table 3). This tight connection and positive relationship between diatoms (*r*-strategist with superior phosphorus kinetics) and cladocerans (P-rich animals) deviate from the conceptualization postulated by Lampert and Sommer (1997), where they hypothesized that zooplankton monotonically decreases the biomass of highly edible algae but this decrease is at first slow and then becomes faster as zooplankton biomass increases (Lampert and Sommer, 1997, Fig. 6.18, p. 201). In our simulations, the diatom–zooplankton relationship has a positive slope until phosphorus limitation is alleviated and a global maximum is reached, then the net growth rate is negative and the diatom biomass declines (Fig. 8).

Our analysis also suggests that the other two functional groups do not seem to benefit from the phosphorus flux emanating from zooplankton and their summer biomass levels are primarily determined by the external nutrient enrichment conditions along with their phosphorus kinetics or metabolic losses (Tables 4 and 5; Figs. 5 and 6). Interestingly, the classification tree analysis did not provide evidence of a significant negative impact of zooplankton grazing on green algae/cyanobacteria. The latter finding may suggests that the establishment of a closed loop between P-limited diatoms and summer zooplankton community seems to alleviate the other two functional groups from the control exerted by the herbivorous grazing. The weak linkage between green algae/cyanobacteria and zooplankton is further promoted by the way the zooplankton feeding selectivity is modelled, i.e., food selection is determined by prior assigned preferences of the two zooplankton groups but also changes dynamically as a function of the relative availability of the four food-types: diatoms, green algae, cyanobacteria, and detritus (Fasham et al., 1990; Arhonditsis and Brett, 2005a). Therefore, having consistently higher concentrations, the diatoms are the most favourable food and are selectively ingested throughout the annual cycle. Finally, another interesting aspect of the primary producer–herbivore interface was investigated in an earlier study by

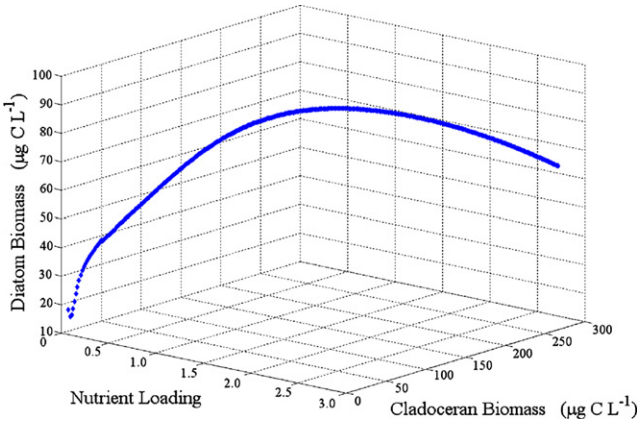

Fig. 8 – The diatom–cladocerans relationship during the summer-stratified period across a wide range of nutrient loading corresponding to the 1–300% of the current total organic carbon, total nitrogen and total phosphorus input concentrations in Lake Washington.

Arhonditsis and Brett (2005b), where a wide variety of pulses were induced to test the resilience of the phytoplankton community to disturbances that resemble episodic mixing events during the summer-stratified period. Generally, the planktonic community was quite resistant and no major structural shifts were observed from the hypolimnetic nutrient intrusions; just minor phytoplankton peaks that were proportionally allocated among the three phytoplankton groups. Transient nutrient pulses are thought to induce competitive advantages for storage strategists, e.g., the cyanobacteria functional group in the present model (Suttle et al., 1987), and such structural shifts were obtained only when cladocerans were eliminated from the system. This result was interpreted as evidence that the dominant grazers act as a ''safety valve'' and do not allow cyanobacteria to gain competitive advantage. Recent experimental studies reported similar results supporting the hypothesis that large-bodied zooplankton grazers have the ability to reduce phytoplankton sensitivity to external perturbations (Cottingham and Schindler, 2000; Cottingham et al., 2004).

5. Conclusions and future perspectives

We used a complex aquatic biogeochemical model to elucidate phytoplankton competition patterns under nutrient enrichment conditions. Because complex models project species competition onto a higher number of niche dimensions, we were able to simultaneously examine the role of functional properties, abiotic conditions, and food-web interactions on the structural shifts observed in phytoplankton communities. Our analysis provided evidence that the intergroup variability in the minimum cell quota and maximum transport rate at the cell surface for phosphorus along with the group-specific metabolic losses can shape the structure of phytoplankton communities. We also found a tight connection and positive relationship between diatoms (fast-growing species with superior phosphorus kinetics) and cladocerans (P-rich animals) that seems to reduce the grazing pressure exerted on the other residents of the phytoplankton community. Our model also supports the hypothesis that large herbivorous animals buffer the effects of external perturbations (e.g., nutrient pulses) on the phytoplankton community structure.

From an ecological standpoint, the robustness of some of our findings can be further examined if we adopt the most realistic assumption of a higher niche overlap when characterizing the functional attributes of the modelled groups (Seip and Reynolds, 1995). Generally, the probability distributions characterizing the functional properties of the biotic entities modelled is a critical feature of the present framework (Fig. 1), and the recognition of their importance does invite one to ask if there are any operational rules to determine the species optimal spacing and niche width along the different niches' axes of the simulated habitats. We believe that the primary factor is the selection of coherent species assemblages that demonstrate distinctive ecologies and recurring patterns in the system being studied. In particular, Reynolds et al.'s (2002) and Reynolds' (2006) functional classification scheme provides an excellent guide for designing functional groups with behavioural/physiological features that can be translated into realistic probability distributions. Our fidelity on the phytoplankton community modelled can then be tested by assessing the sensible behaviour exhibited by the different phytoplankton assemblages across different gradients of the simulated habitat, e.g., enrichment conditions, climate change. Thus, model dysfunctionality should be used to dictate the most reliable structure of the biotic communities, e.g. optimal number and organizational level (species, genera, taxa) of the biotic entities modelled along with the components of physiology or other ecological processes needed. The latter issue highlights the importance of improving the mathematical representation of phytoplankton adaptive strategies for resources procurement to effectively link variability at the organismal level with ecosystem-scale patterns. For example, one of the most controversial features of aquatic biogeochemical models is the mathematical formulation used for describing interactions among multi-nutrients, light, and temperature (Flynn, 2003). Several authors pinpoint the inadequacy of the Monod or the Droop version of the quota model for simulating multi-nutrient interactions and transient states (e.g., Davidson and Cunningham, 1996; Flynn, 2003). While several recent mechanistic submodels have significantly improved the sophistication level (Legovic and Cruzado, 1997; Geider et al., 1998; Flynn, 2001), the substantial increase of complexity has been a major impediment for their incorporation in ecosystem models. The ongoing debate on the need to balance between simplicity and realism (Anderson, 2005; Flynn, 2005; Arhonditsis et al., 2006) should identify the best strategies (e.g., prudent increase in complexity, rigorous error analysis) for developing reliable modeling tools that can assist the management of natural resources and also contribute to the development of ecological theories.

Acknowledgments

Funding for this study was provided by the UTSC Research Fellowships (Master of Environmental Science Program, Centre for Environment & University of Toronto at Scarborough) and the Connaught Committee (University of Toronto, Matching Grants 2006–2007).

REFERENCES

Anderson, T.R., 2005. Plankton functional type modelling: running before we can walk? J. Plankton Res. 27, 1073–1081.

Arhonditsis, G.B., Brett, M.T., 2004. Evaluation of the current state of mechanistic aquatic biogeochemical modeling. Mar. Ecol. Prog. Ser. 271, 13–26.

Arhonditsis, G.B., Brett, M.T., 2005a. Eutrophication model for Lake Washington (USA) Part I. Model description and sensitivity analysis. Ecol. Model. 187, 140–178.

Arhonditsis, G.B., Brett, M.T., 2005b. Eutrophication model for Lake Washington (USA) Part II. Model calibration and system dynamics analysis. Ecol. Model. 187, 179–200.

Arhonditsis, G.B., Tsirtsis, G., Karydis, M., 2002. The effects of episodic rainfall events to the dynamics of coastal marine ecosystems: applications to a semi-enclosed gulf in the Mediterranean Sea. J. Mar. Syst. 35, 183–205.

Arhonditsis, G.B., Winder, M., Brett, M.T., Schindler, D.E., 2004. Patterns and mechanisms of phytoplankton variability in Lake Washington (USA). Water Res. 38, 4013–4027.

Arhonditsis, G.B., Adams-VanHarn, B.A., Nielsen, L., Stow, C.A., Reckhow, K.H., 2006. Evaluation of the current state of mechanistic aquatic biogeochemical modeling: citation analysis and future perspectives. Environ. Sci. Technol. 40, 6547–6554.

Arhonditsis, G.B., Paerl, H.W., Valdes-Weaver, L.M., Stow, C.A., Steinberg, L.J., Reckhow, K.H., 2007. Application of Bayesian structural equation modeling for examining phytoplankton dynamics in the Neuse River Estuary (North Carolina, USA). Estuar. Coast. Shelf Sci. 72, 63–80.

Baines, S.B., Pace, M.L., 1991. The production of dissolved organic-matter by phytoplankton and its importance to bacteria – patterns across marine and fresh-water systems. Limnol. Oceanogr. 36, 1078–1090.

Boersma, M., 1995. Competition in natural populations of *Daphnia*. Oecologia 103, 309–318.

Breiman, L., Friedman, J.H., Olshen, R.A., Stone, C.J., 1984. Classification and Regression Trees. Wadsworth International Group, Belmont, CA, 358 pp.

Brett, M.T., Arhonditsis, G.B., Mueller, S.E., Hartley, D.M., Frodge, J.D., Funke, D.E., 2005. Non-point-source impacts on stream nutrient concentrations along a forest to urban gradient. Environ. Manag. 35, 330–342.

Cerco, C.F., Cole, T.M., 1994. CE-QUAL-ICM: a Three-dimensional Eutrophication Model, Version 1.0. User's Guide. US Army Corps of Engineers Waterways Experiments Station, Vicksburg, MS.

Chen, C., Ji, R., Schwab, D.J., Beletsky, D., Fahnenstiel, G.L., Jiang, M., Johengen, T.H., Vanderploeg, H., Eadie, B., Budd, J.W., Bundy, M.H., Gardner, W., Cotner, J., Lavrentyev, P.J., 2002. A model study of the coupled biological and physical dynamics in Lake Michigan. Ecol. Model. 152, 145–168.

Costanza, R., Sklar, F.H., 1985. Articulation, accuracy and effectiveness of mathematical models – a review of freshwater wetland applications. Ecol. Model. 27, 45–68.

Cottingham, K.L., Carpenter, S.R., 1998. Population, community, and ecosystem variates as ecological indicators: phytoplankton responses to whole-lake enrichment. Ecol. Appl. 8, 508–530.

Cottingham, K.L., Schindler, D.E., 2000. Effects of grazer community structure on phytoplankton response to nutrient pulses. Ecology 81, 183–200.

Cottingham, K.L., Glaholt, S., Brown, A.C., 2004. Zooplankton community structure affects how phytoplankton respond to nutrient pulses. Ecology 85, 158–171.

Davidson, K., Cunningham, A., 1996. Accounting for nutrient processing time in mathematical models of phytoplankton growth. Limnol. Oceanogr. 41, 779–783.

De'ath, G., Fabricius, K.E., 2000. Classification and regression trees: a powerful yet simple technique for ecological data analysis. Ecology 81, 3178–3192.

Doveri, F., Scheffer, M., Rinaldi, S., Muratori, S., Kuznetsov, Y., 1993. Seasonality and chaos in a plankton-fish model. Theor. Popul. Biol. 43, 159–183.

Elser, J.J., Foster, D.K., 1998. N:P stoichiometry of sedimentation in lakes of the Canadian shield: relationships with seston and zooplankton elemental composition. Ecoscience 5, 56–63.

Fasham, M.J.R., Ducklow, H.W., McKelvie, S.M., 1990. A nitrogen-based model of plankton dynamics in the oceanic mixed layer. J. Mar. Res. 48, 591–639.

Ferris, J.M., Christian, R., 1991. Aquatic primary production in relation to microalgal responses to changing light – a review. Aquat. Sci. 53, 187–217.

Floder, S., Sommer, U., 1999. Diversity in planktonic communities: an experimental test of the intermediate disturbance hypothesis. Limnol. Oceanogr. 44, 1114–1119.

Flynn, K.J., 2001. A mechanistic model for describing dynamic multi-nutrient, light, temperature interactions in phytoplankton. J. Plankton Res. 23, 977–997.

Flynn, K.J., 2003. Modeling multi-nutrient interactions in phytoplankton; balancing simplicity and realism. Prog. Oceanogr. 56, 249–279.

Flynn, K.J., 2005. Castles built on sand: dysfunctionality in plankton models and the inadequacy of dialogue between biologists and modellers. J. Plankton Res. 27, 1205–1210.

Flynn, K.J., 2006. Reply to Horizons Article 'Plankton functional type modelling: running before we can walk' Anderson (2005): II. Putting trophic functionality into plankton functional types. J. Plankton Res. 28, 873–875.

Franks, P.J.S., 2002. NPZ models of plankton dynamics: their construction, coupling to physics, and application. J. Oceanogr. 58, 379–387.

Geider, R.J., MacIntyre, H.L., Kana, T.M., 1998. A dynamic regulatory model of phytoplankton acclimation to light, nutrients and temperature. Limnol. Oceanogr. 43, 679–694.

Grover, J.P., 1991. Resource competition in a variable environment – phytoplankton growing according to the variable-internal-stores model. Am. Nat. 138, 811–835.

Grover, J.P., 1997. Resource Competition. Chapman and Hall, London, 342 pp.

Hamilton, D.P., Schladow, S.G., 1997. Prediction of water quality in lakes and reservoirs Part I. Model description. Ecol. Model. 96, 91–110.

Hansson, L.A., Annadotter, H., Bergman, E., Hamrin, S.F., Jeppesen, E., Kairesalo, T., Luokkanen, E., Nilsson, P.A., Sondergaard, M., Strand, J., 1998. Biomanipulation as an application of food chain theory: constraints, synthesis and recommendations for temperate lakes. Ecosystems 1, 558–574.

Hardin, G., 1960. The competitive exclusion principle. Science 131, 1292–1297.

Hastings, A., Powell, T., 1991. Chaos in a three-species food chain. Ecology 72, 896–903.

Heaney, S.I., Lund, J.W.G., Canter, H.M., Gray, K., 1988. Population dynamics of *Ceratium* spp. in three English lakes, 1945–1985. Hydrobiologia 161, 133–148.

Huisman, J., Oostveen, P., Weissing, F.J., 1999. Critical depth and critical turbulence: two different mechanisms for the development of phytoplankton blooms. Limnol. Oceanogr. 44, 1781–1787.

Hutchinson, G.E., 1961. The paradox of the plankton. Am. Nat. 95, 137–145.

Jassby, A.D., 1999. Uncovering mechanisms of interannual variability from short ecological time series. In: Scow, K.M., Fogg, G.E., Hinton, D.E., Johnson, M.L. (Eds.), Integrated Assessment of Ecosystem Health. CRC Press, Boca Raton, FL, pp. 285–306.

Jassby, A.D., Platt, T., 1976. Mathematical formulation of the relationship between photosynthesis and light for phytoplankton. Limnol. Oceanogr. 21, 540–547.

Jorgensen, S.E., 1999. State-of-the-art of ecological modeling with emphasis on development of structural dynamic models. Ecol. Model. 120, 75–96.

Jorgensen, S.E., Bendoricchio, G., 2001. Fundamentals of Ecological Modelling, third ed. Elsevier, Amsterdam, 530 pp.

Jorgensen, S.E., Nielsen, S.N., Jorgensen, L.A., 1991. Handbook of Ecological Parameters and Ecotoxicology. Pergamon Press, Amsterdam, 1263 pp.

Karolyi, G., Pentek, A., Scheuring, I., Tel, T., Toroczkai, Z., 2000. Chaotic flow: the physics of species coexistence. Proc. Natl. Acad. Sci. U. S. A. 97, 13661–13665.

Kuznetsov, Y.A., 1995. Elements of Applied Bifurcation Theory. Springer-Verlag, New York, NY, 591 pp.
Lampert, W., Sommer, U., 1997. Limnoecology. Oxford University Press, Oxford, 382 pp.
Lawton, J.H., 1997. The role of species in ecosystems: aspects of ecological complexity and biological diversity. In: Abe, T., Levin, S.R., Higashi, M. (Eds.), Biodiversity: an Ecological Perspective. Springer-Verlag, New York, NY, pp. 215–228.
Le Quere, C., 2006. Reply to Horizons Article 'Plankton functional type modelling: running before we can walk' Anderson (2005): I. Abrupt changes in marine ecosystems? J. Plankton Res. 28, 871–872.
Legendre, P., Legendre, L., 1998. Numerical Ecology, second ed. Elsevier Science B.V., Amsterdam, 853 pp.
Legovic, T., Cruzado, A., 1997. A model of phytoplankton growth on multiple nutrients based on the Michaelis–Menten–Monod uptake, Droop's growth and Liebig's law. Ecol. Model. 99, 19–31.
Lessard, E.J., Merico, A., Tyrrell, T., 2005. Nitrate: phosphate ratios and *Emiliania huxleyi* blooms. Limnol. Oceanogr. 50, 1020–1024.
Levin, S.A., 1992. The problem of pattern and scale in ecology. Ecology 73, 1943–1967.
Levins, R., 1966. The strategy of model building in population biology. Am. Sci. 54, 421–431.
Litchman, E., 1998. Population and community responses of phytoplankton to fluctuating light. Oecologia 117, 247–257.
Marshal, T.C., Peters, R.H., 1989. General patterns in the seasonal development of chlorophyll *a* for temperate lakes. Limnol. Oceanogr. 34, 856–867.
Omlin, M., Brun, P., Reichert, P., 2001. Biogeochemical model of Lake Zurich: sensitivity, identifiability and uncertainty analysis. Ecol. Model. 141, 105–123.
Padisak, J., Reynolds, C.S., Sommer, U. (Eds.), 1993. Intermediate Disturbance Hypothesis in Phytoplankton Ecology-Foreword. Kluwer Academic Publishers, Dordrecht, 199 pp.
Paine, R.T., 1966. Food web complexity and species diversity. Am. Nat. 100, 65–75.
Reynolds, C.S., 1993. Scales of disturbance and their role in plankton ecology. Hydrobiologia 249, 157–171.
Reynolds, C.S., 2006. The Ecology of Phytoplankton. Cambridge University Press, Cambridge, 535 pp.
Reynolds, C.S., Huszar, V., Kruk, C., Naselli-Flores, L., Melo, S., 2002. Towards a functional classification of the freshwater phytoplankton. J. Plankton Res. 24, 417–428.
Richman, M.B., 1986. Rotation of principal components. Int. J. Climatol. 6, 293–335.
Rothhaupt, K.O., 2000. Plankton population dynamics: food web interactions and abiotic constraints. Freshw. Biol. 45, 105–109.
Sandgren, C.D., 1991. Growth and Reproductive Strategies of Freshwater Phytoplankton. Cambridge University Press, Cambridge, 442 pp.
Scheffer, M., Van Nes, E.H., 2006. Self-organized similarity, the evolutionary emergence of groups of similar species. Proc. Natl. Acad. Sci. U. S. A. 103, 6230–6235.
Scheffer, M., Rinaldi, S., Huisman, J., Weissing, F.J., 2003. Why plankton communities have no equilibrium: solutions to the paradox. Hydrobiologia 491, 9–18.
Schladow, S.G., Hamilton, D.P., 1997. Prediction of water quality in lakes and reservoirs Part II. Model calibration, sensitivity analysis and application. Ecol. Model. 96, 111–123.
Seip, K.L., Reynolds, C.S., 1995. Phytoplankton functional attributes along trophic gradient and season. Limnol. Oceanogr. 40, 589–597.
Simon, H.A., 2001. Science seeks parsimony, not simplicity: searching for pattern in phenomena. In: Zellner, A., Keuzenkamp, H.A., McAleer, M. (Eds.), Simplicity, Inference and Modelling: Keep It Sophisticatedly Simple. Cambridge University Press, Cambridge, pp. 32–72.
Sommer, U., Gliwicz, Z.M., Lampert, W., Duncan, A., 1986. The plankton-ecology-group model of seasonal succession of planktonic events in fresh waters. Arch. Hydrobiol. 106, 433–471.
Suttle, C.A., Stockner, J.G., Harrison, P.J., 1987. Effects of nutrient pulses on community structure and cell-size of a freshwater phytoplankton assemblage in culture. Can. J. Fish. Aquat. Sci. 44, 1768–1774.
Tilman, D., 1982. Resource Competition and Community Structure. Princeton University Press, Princeton, NJ, 296 pp.
Turpin, D.H., 1988. Physiological mechanisms in phytoplankton resource competition. In: Sandgren, C.D. (Ed.), Growth and Reproductive Strategies of Freshwater Phytoplankton. Cambridge University Press, New York, NY, pp. 316–368.
Tyrrell, T., Merico, A., 2004. *Emiliania huxleyi*: bloom observations and the conditions that induce them. In: Thierstein, H.R., Young, J.R. (Eds.), Coccolithophores: from Molecular Processes to Global Impact. Springer-Verlag, Berlin, pp. 75–97.
Van Nes, E.H., Scheffer, M., 2005. A strategy to improve the contribution of complex simulation models to ecological theory. Ecol. Model. 185, 153–164.
Vanni, M.J., Temte, J., 1990. Seasonal patterns of grazing and nutrient limitation of phytoplankton in a eutrophic lake. Limnol. Oceanogr. 35, 697–709.
Wetzel, R.G., 2001. Limnology: Lake and River Ecosystems, third ed. Academic Press, New York, NY, 1006 pp.